Electrochemical removal of nitrate from waste water

PhD Thesis

Summary

Florina Maria CUIBUS (b. BĂLAJ)

Scientific Supervisors:

Prof. Univ. Dr. Ing. Petru ILEA
Prof. Univ. Dr. rer. nat. habil. Andreas BUND

Cluj Napoca

2012

TABLE OF CONTENTS

Keywords

Nitrate, nitrite electroreduction, alkaline waste waters, Cu and CuSn electrode, square wave voltammetry, electroactive products detection, electrochemical flow reactor.

LITERATURE REVIEW

1. NITRATES AND THEIR PRESENCE IN THE ECOSYSTEM

To obtain freshwater of high quality directly from the kitchen tap is something that many of us take for granted. We use it every day to prepare our food, to wash our clothes and for many other things. In some places, increasing environmental pollution has made many wells unsuitable as freshwater sources. Use of water treatment techniques is needed in order to meet society's need of high quality water. The regulations on the water quality are continuously getting stricter as modern and more accurate analytical instruments are developed, making it possible to detect lower levels of impurities. The definition of clean water in many industrial applications is completely different compared to the potable water. The microelectronic and pharmaceutical industries require extremely pure water in their processes. In power plants, ultrapure water is used to reduce problems with corrosion that could be a serious issue at the temperatures and pressures present in the heat exchanges. The production of this ultrapure water requires complicated water treatment systems.

Owing to agricultural and industrial activities, the nitrate concentrations levels in surface and groundwater have increased to such an extent that the admitted standards in drinking water have been largely exceeded in many regions in the world.

Various methods such as biological, physicochemical and electrochemical techniques have been proposed for the removal of nitrate from potable and wastewaters. The physicochemical processes such as ion exchange [1], reverse osmosis [2] and electrodialysis [3] produce secondary wastes, because the nitrates are merely separated but not destroyed. The ideal process for nitrate removal would be able to treat large volumes of water at a low cost. Furthermore it is desirable that the process adapts well to different feed loads and works without the addition of any chemicals.

The biological method for the nitrate removal from waste water is the method of choice. In this method, bacteria convert nitrate to non-toxic nitrogen gas with a yield of about 99% [4]. However, there are many types of waste water in which the biological method cannot be applied due to the toxic environment for the bacteria. Such waste waters are those containing toxic organic compounds, heavy metals, high concentration of nitrate or other salts and extreme pH values. Examples of this type of waste waters are the low level nuclear wastes. Therefore, it is a major challenge to develop a complementary method for the treatment of wastes in which the biological method cannot be applied. This technique must combine: high

rate and high selectivity of conversion of nitrate to nitrogen, low operation costs and broad range of applications, regardless of the solution composition.

The various applications of the electrochemical processes are detailed as follows:

- In the electrochemical destruction of sodium nitrate, sodium hydroxide is the major product of the process. If the sodium hydroxide could be recovered and recycled, significant reduction in the quantity of waste requiring disposal would be realized. Immediate use of sodium hydroxide included: neutralization of fresh waste and as a corrosion inhibitor in the waste storage and evaporation facilities [5];

- Electrochemical processes are used for the production of a variety of industrial chemicals like ammonia, nitrogen, hydroxylamine, ammonium hydroxide, sodium hydroxide and oxides of nitrogen;

- Electrochemical methods are also useful for the treatment of waste streams and waters prior to disposal and release to the environment;

- The electrochemical reactions are easily controllable; they can be stopped instantaneously by shutting off the power to the electrochemical reactor;

- Moreover, no additional chemicals are necessary in the process, and therefore, there is minimal or no secondary wastes generated by the process.

In addition, previous investigations showed that the reduction efficiency of nitrate ions depends strongly on the nature of the material used to modify the electrode surface. A series of cathode materials were investigated to establish their performance towards the electrochemical reduction of NO_3^- ions in aqueous solutions. The importance of investigation of multicomponent electrodes is due to the high catalytic activity of noble metals in hydrogenation processes, the first choice for reducing nitrates. The reduction mechanism of the NO_3^- and NO_2^- ions at multi- and monometallic electrode surfaces is very similar, although the activity and selectivity of mixed composites strongly depends on the preparation methods.

2. AIM OF THE THESIS

The electrochemical reduction of nitrate has a high importance mainly for environmental and analytical purposes. During the last years, the interest has been focused on the conversion of nitrate to the non-toxic nitrogen gas from wastes where the biological method cannot be applied. The objective of the current doctoral study is focused on an electrochemical method used for the removal of nitrate from alkaline model nitrate solutions. The electrochemical methods offer a much broader application range in comparison to the biological method.

The personal contributions described in this doctoral thesis are divided in three parts. The first part of the study has been focused on synthesis and characterization of electrode materials which are suitable for ERN. Most of the characterization measurements have been proposed to collect additional information helpful to obtain a range of electroplating conditions in which adherent and uniform coatings can be produced. The deposits will serve as an electrode material/electrocatalysts in ERN. A number of supplementary techniques, including scanning electron microscopy and X-ray spectroscopy were used to provide a better view on the structural characterization of the deposits.

The second part of the study deals with an electrochemical method for monitoring / determining easy and quickly the species resulting from ERN. Square-wave voltammetry and cyclic hydrodynamic voltammetry are known to be powerful analytical tools. In the same time, the rotating ring-disc electrode technique is also an important electrochemical approach for the detection of reaction intermediates.

The last part of the thesis deals with the reduction of nitrates in an electrochemical flow cell. The cell was operated in a divided configuration, to remove possible interferences such as nitrite oxidation at the anode. Constant current electrolyses were performed using various cathode materials and a model nitrate solution. The concentration of nitrate and nitrite were monitored during the electroreduction process. The apparent rate constants, the influence of flow rate, current efficiencies and energy consumptions, were evaluated within this chapter. Moreover, a comparison of the two electrode materials was performed.

PERSONAL CONTRIBUTIONS
3. SYNTHESIS OF ELECTRODE MATERIALS

Previous investigations showed that the reduction efficiency of nitrate ions depends strongly on the nature of the electrode material. The interest for copper-tin alloys coatings increased in the last years due to their better corrosion and mechanical properties compared with those of pure copper or tin coatings. There is a worldwide tendency in substitution of cadmium and lead that are intensively used in the ERN process, due to their toxicity.

Copper has the highest electrocatalytic effect among transition-metal monometallic electrodes for the cathodic reduction of nitrate ions in acid and also in alkaline media [6]. Tin represents itself an efficient electrocatalyst for the reduction of nitrate as described by Katsouranos et al. [7]. Also, Sn has positive effect on electrocatalytic activity when is added to Cu as a base cathode material in the composition region up to 10 wt.% [8]. The group of Polatides [9] claimed that by using a CuSn electrode at very negative potentials (E = -2 V *vs*. Ag/AgCl) nitrate can be 97% removed with a selectivity of 35% towards N_2 as the final product. Based on the literature study, we consider that copper, tin and copper-tin alloy have to be further studied due to their properties and applications in the ERN process.

3.1. Cu and Sn electrodeposition

3.1.1. Cyclic voltammetry analysis

Cyclic voltammetry measurements were carried out at a platinum disc electrode. The method was applied in order to find the region where the Cu and Sn depositions take place. The electrode potential was linearly swept from +0.1V to −0.8V *vs.* $Ag/AgCl/KCl_{sat}$ then the sweep direction was reversed at various potential sweep rates (10, 20, 40, 80 and 160 mVs^{-1}). Three different sets of copper and tin concentrations were used in this study. Figure 5.3 shows the cyclic voltammogram of copper at a platinum surface in a sulphuric acid electrolyte.

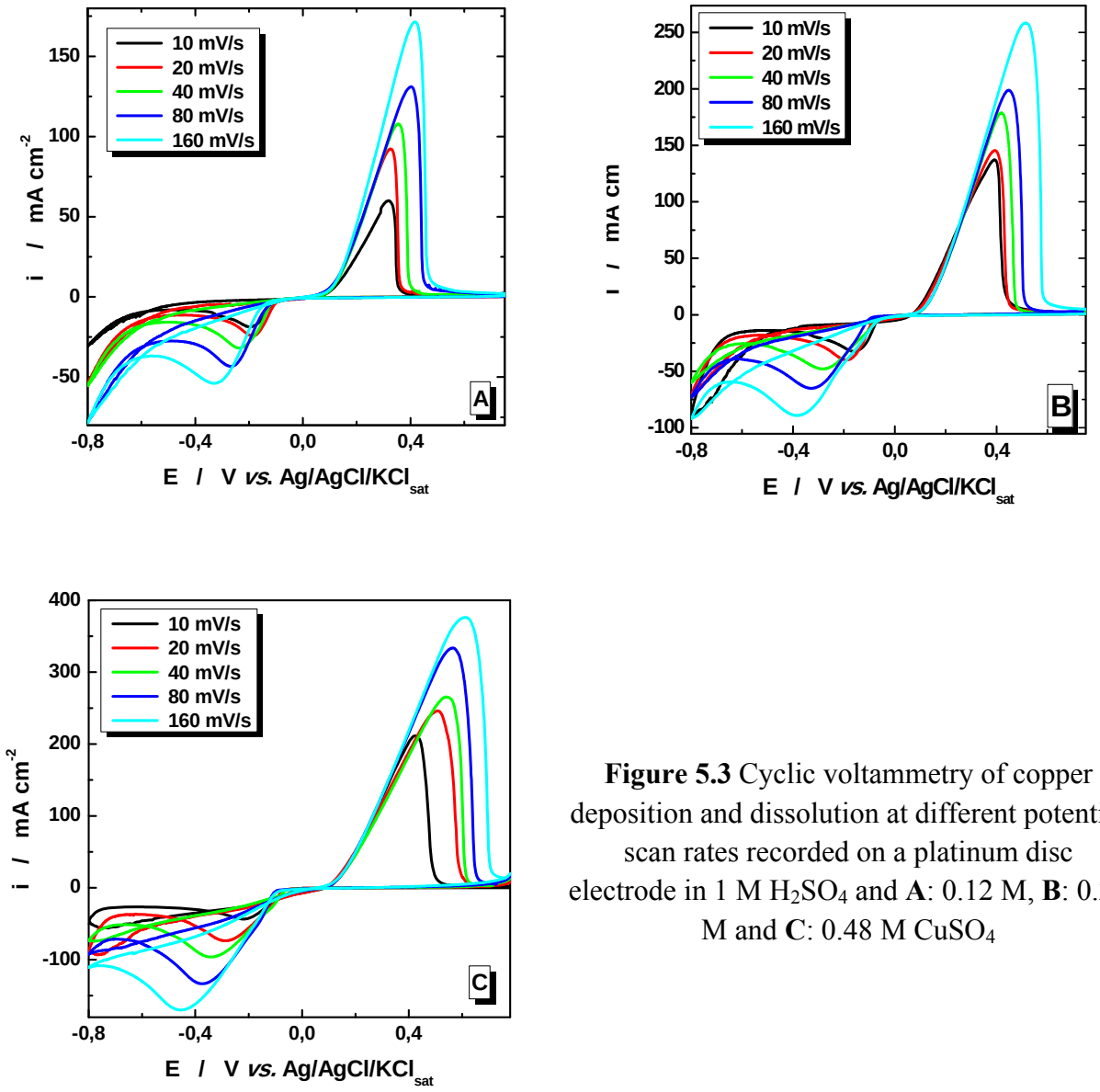

Figure 5.3 Cyclic voltammetry of copper deposition and dissolution at different potential scan rates recorded on a platinum disc electrode in 1 M H_2SO_4 and **A**: 0.12 M, **B**: 0.24 M and **C**: 0.48 M $CuSO_4$

In a similar series of experiments, Sn deposition was investigated. The influence of the scan rate on tin deposition is presented in Figure 5.4.

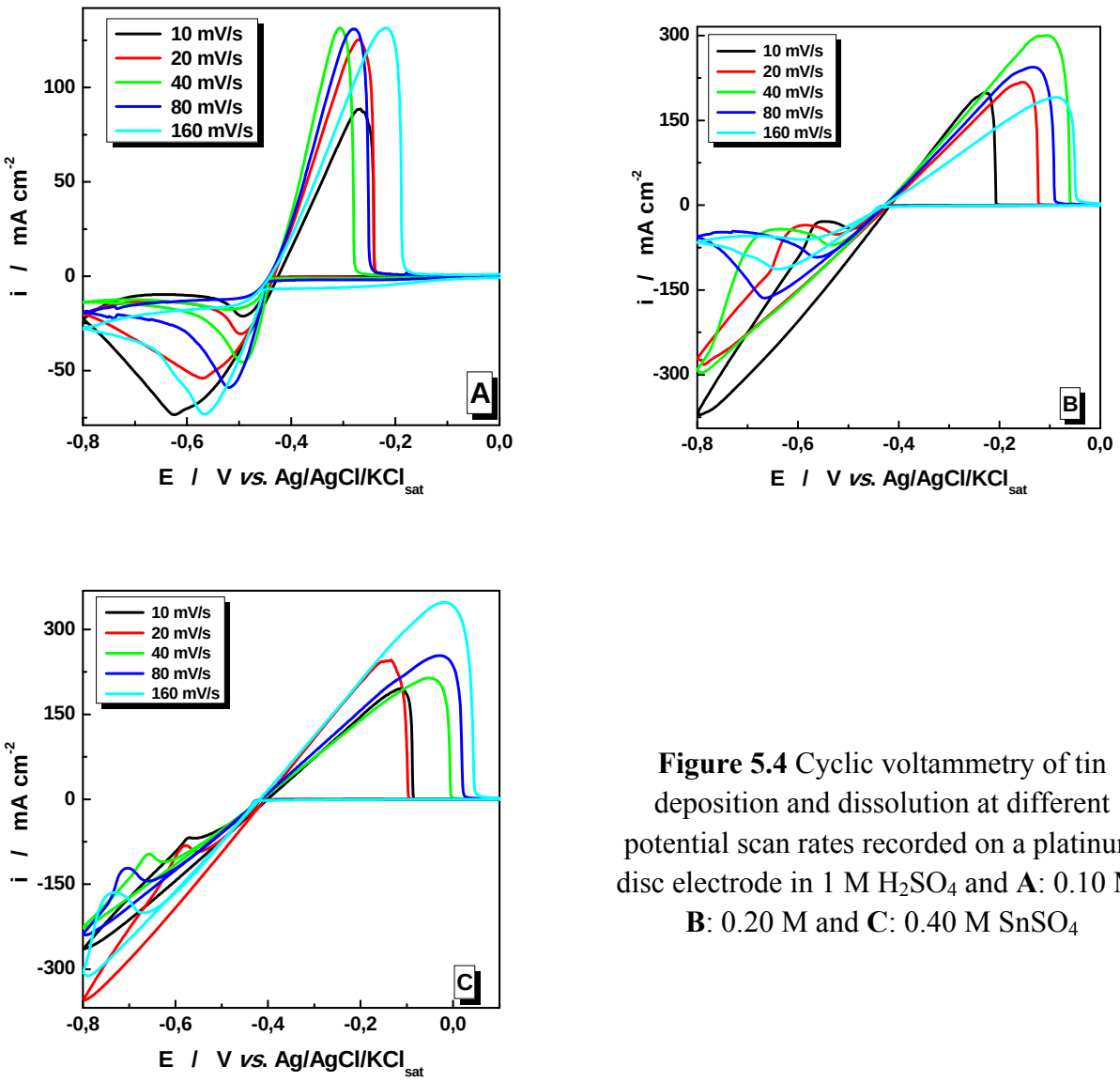

Figure 5.4 Cyclic voltammetry of tin deposition and dissolution at different potential scan rates recorded on a platinum disc electrode in 1 M H_2SO_4 and **A**: 0.10 M, **B**: 0.20 M and **C**: 0.40 M $SnSO_4$

The peak current density is associated with the complete consumption of cupric ions (Fig. 5.3) and stannous ions (Fig. 5.4) at the electrode surface under mass transport control. On reversing the potential sweep from −0.8V to +0.1V *vs.* $Ag/AgCl/KCl_{sat}$ a single stripping peak was observed, confirming the two-electron oxidation of metallic copper to cupric ions (see Fig. 5.3) and oxidation of metallic tin to stannous ions (see Fig. 5.4) via the reverse of the reactions 5.1 and 5.2. The deposition of copper and tin at the platinum surface is evidenced by the sharp rise in the current at a potential of approximately −0.30V *vs.* $Ag/AgCl/KCl_{sat}$ (for copper deposition) and at about −0.5V *vs.* $Ag/AgCl/KCl_{sat}$ (for tin deposition).

At potentials more negative than -0.5V vs. $Ag/AgCl/KCl_{sat}$ (in the case of Cu) and -0.7V vs. $Ag/AgCl/KCl_{sat}$ (in the case of Sn) water decomposition occurs. This reaction implies the occurrence of hydrogen evolution and of the OH^- species on the cathode surface. As a

consequence, the formation of metal hydroxides can occur and they can precipitate on the electrode and together with the hydrogen evolution could block the electrode surface and inhibit further depositions. After the region where the water decomposition occurs, the probability of forming oxide inhibiting species is higher, therefore, the deposition will be delayed when the sweeping of the potential is made in the anodic direction.

Cyclic voltamogramms were performed at different concentrations of Cu and Sn in the bath solution.

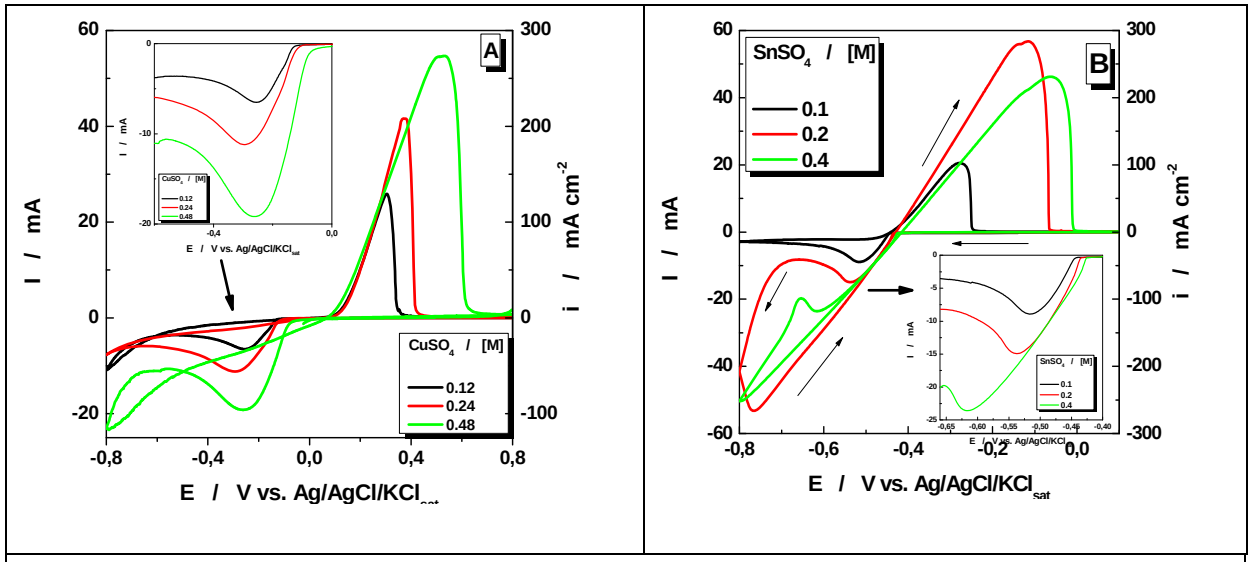

Figure 5.5 Influence of copper (**A**) and tin (**B**) concentrations on the corresponding peak currents. Experimental conditions: platinum disc electrode (S = 0.2 cm^2), scan rate: 50 mV s^{-1}. The electrolyte was prepared at 296 K and contains 1 M H_2SO_4

Analyzing the voltamogramms (Fig. 5.5) and the data from Table 5.2 we can conclude that the anodic and cathodic Cu peaks (Fig. 5.5A) and Sn peaks (Fig. 5.5B) do not represent the mirror image of one another, and they characterize a quasi-reversible process. The cathodic peaks are shifted to more negative potentials as the concentration and the scan rate increases. The peak potential difference, $\Delta\varepsilon$, ranged between 126 and 156 mV for copper ions.

Table 5.2: Electrochemical parameters corresponding to voltammetric response of the electrode (experimental conditions as in Fig.5.5)

Electrolyte	$E^{0'}$ (mV *vs.*Ag/AgCl)	Δε(mV)	I_{pa}/I_{pc}
$CuSO_4$ 0.12 M	320	126	2.88
$CuSO_4$ 0.24 M	349	130	2.97
$CuSO_4$ 0.48 M	534	156	2.20
$SnSO_4$ 0.10 M	398	238	2.30
$SnSO_4$ 0.20 M	327	422	3.80
$SnSO_4$ 0.40 M	339.5	555	1.96

The number of electrons involved in the reaction can be determined by [10]:

$$i_p = 0.496 \cdot (\alpha z_c)^{1.5} \cdot z \cdot F \cdot A \cdot c \cdot [(F \cdot D \cdot v)/RT]^{0.5} \quad (5.5)$$

where:

i_p is the peak current, z is the number of electrons involved in the electrode reaction, α is the charge transfer coefficient, z_c is the number of electrons transferred in the rate determining step, A is the electrode area surface, D is the diffusion coefficient of stannous ions, v is the potential scan rate and c is the concentration. From the literature data, the diffusion coefficient of stannous ions was estimated to be $6.5\times10^{-10} m^2\ s^{-1}$ [11] and for cupric ions was estimated to be $0.72\times10^{-9}\ m^2 s^{-1}$ [12].

A plot of the peak current i_p as a function of the square root of the scan rate $v^{1/2}$ is shown in Figure 5.6. This plot yields a straight line and from the slope, z the number of electrons involved in the reaction was estimated.

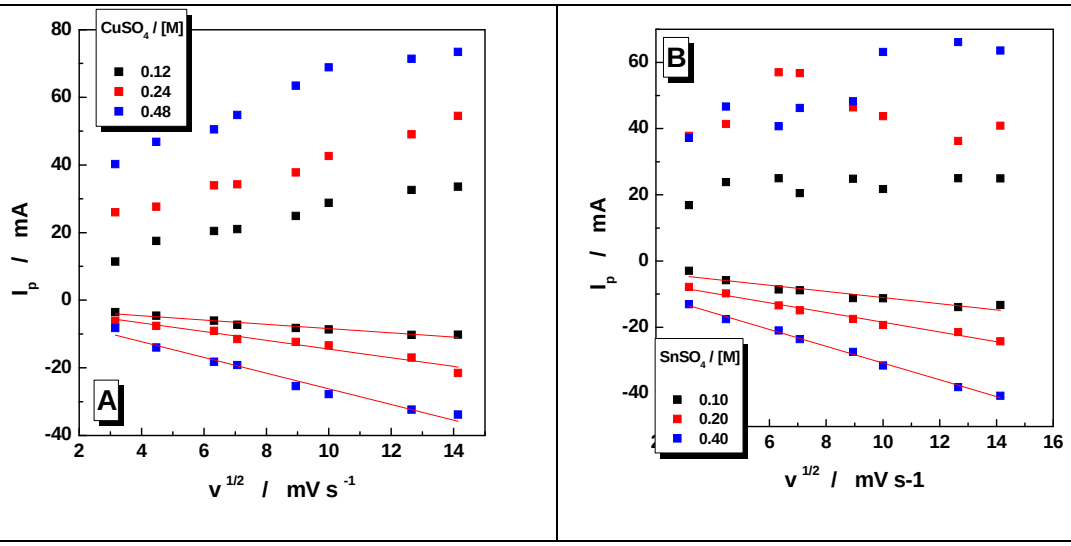

Figure 5.6 Dependence of the peak currents for copper (**A**) and tin (**B**) on the square root of the scan rate $v^{1/2}$ extracted from cyclic voltammograms at a Pt electrode in (A) 0.12 M $CuSO_4$ + 1M H_2SO_4 and (B) 0.10 M $SnSO_4$ + 1M H_2SO_4

For three different copper concentrations (0.12, 0.24 and 0.48 M) *z* was found to be 2.1 ± 0.15. In a similar way, for three different tin concentrations (0.10, 0.20 and 0.40 M), the number of electrons (z =2.2 ± 0.06) involved in the reaction was calculated. According to different possible pathways for the copper and tin electroreduction, only one reaction involves two electrons, which is the reduction of Cu^{2+} and Sn^{2+} to Cu and Sn metallic, respectively.

3.1.2. Morphological studies

3.1.2.1. Study of copper deposits

In order to study the electrodeposition of the copper (as standard electrodeposition process), deposits were obtained galvanostatically from a 0.1 M $CuSO_4$ in 1M H_2SO_4 electrolyte. The SEM images obtained for copper deposits are presented in Figure 5.10.

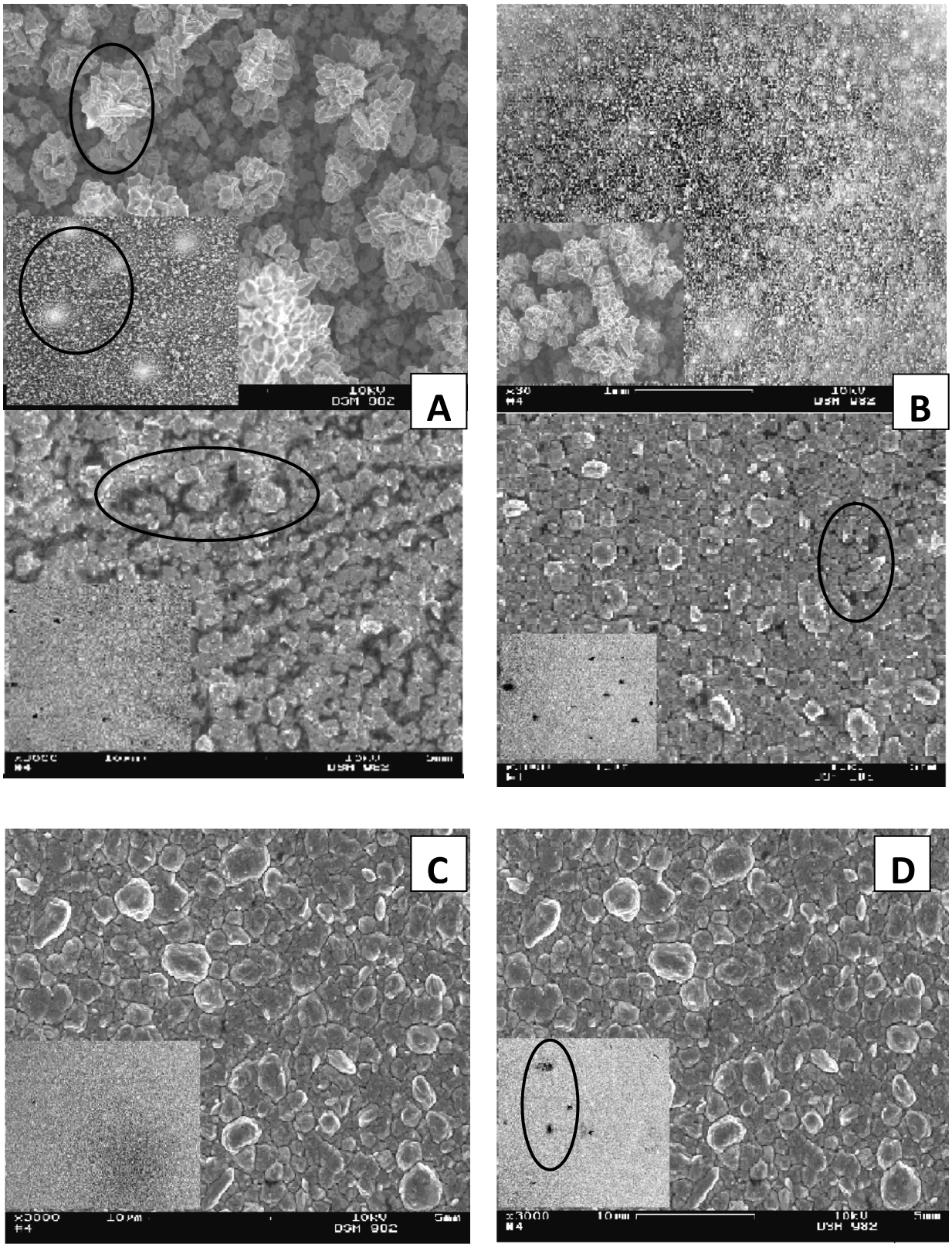

Figure 5.10 SEM micrographs showing the surface morphologies of Cu films obtained at i = 10 mA cm^{-2} (**A**), 20 mA cm^{-2} (**B**), 40 mA cm^{-2} (**C**), 80 mA cm^{-2} (**D**) with (2000 rpm) and without stirring (0 rpm)**.** The large Figures present a x3000 and a x50 (inset) magnification

From Figure 5.10 it can be seen that there are large differences between the deposits obtained with and without stirring the disk electrode. During electrodeposition, bubbles are visible on the cathode surface and dendritic features are produced in the deposits. Deposits of Cu obtained without stirring present crystals of well-defined morphology, some of them elongated with dendritic morphology [13].

On the other hand, at the rotating the disk electrode, a good improvement of the morphology is observed and a smoother surface is obtained. Also, some dark black spots were observed on the surface, suggesting that the surface was not covered entirely by the deposit. Compared to the coatings obtained under static conditions, these deposits are more uniform. SEM micrographs of electrodeposited copper show that smoother surfaces are obtained with a current density of 40 mA cm^{-2}. These results are in accordance with literature [14].

3.1.2.2. Study of tin deposits

Electrodeposition of tin was carried out only at rotating electrodes. In this study the tin deposits were obtained in a simple acidic electrolyte containing 0.10 M $SnSO_4$ and 1M H_2SO_4. The SEM images obtained for tin electrodeposition at different current densities are presented in Figure 5.11.

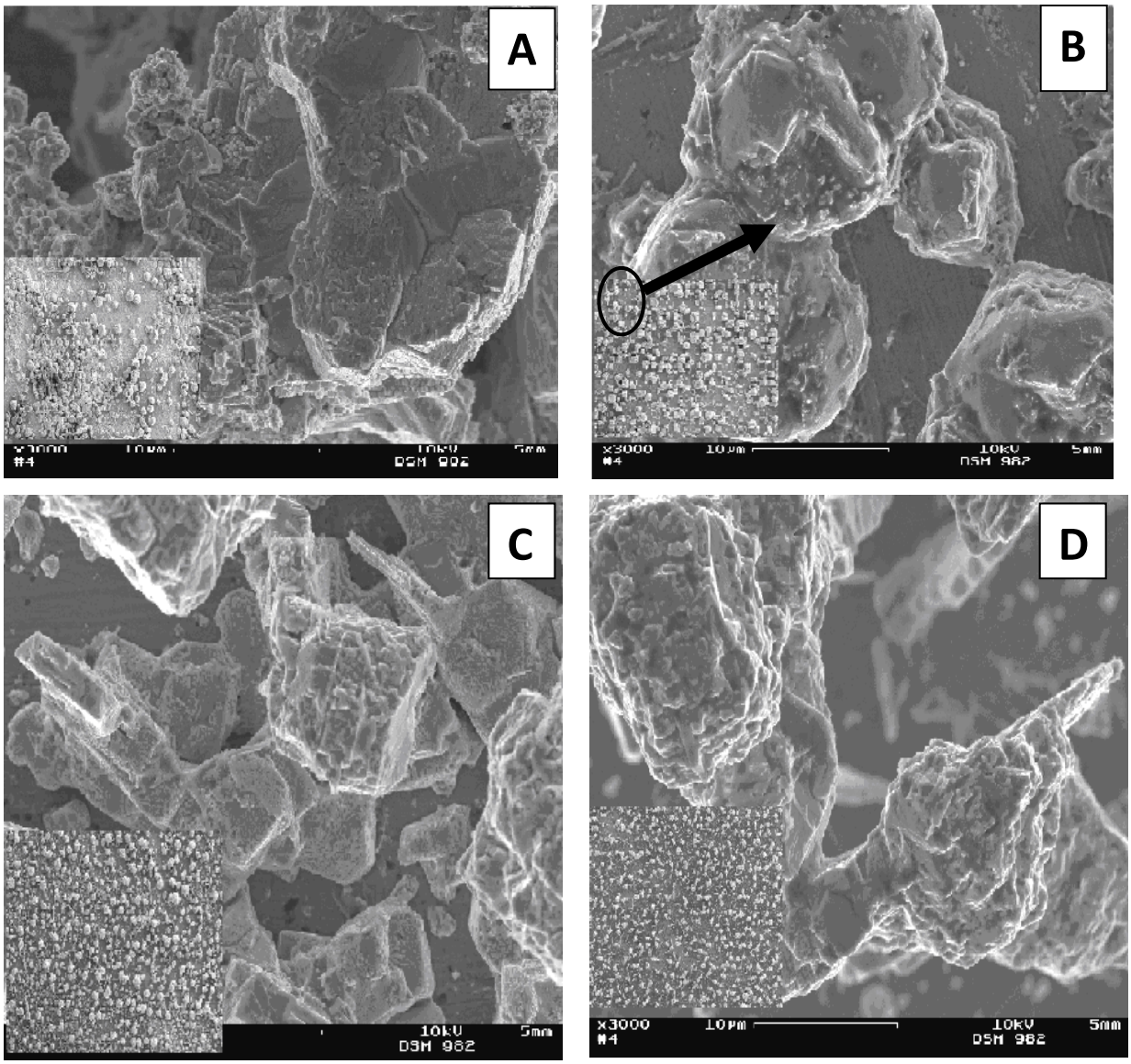

Figure 5.11 SEM micrographs showing the surface morphologies of Sn films obtained at i = 10 mA cm^{-2} (**A**), 20 mA cm^{-2} (**B**), 40 mA cm^{-2} (**C**), 80 mA cm^{-2} (**D**) with (2000 rpm) stirring. (x 3000 and x 50 inset image, respectively)

From the SEM micrographs (Fig. 5.11) it can be observed that by increasing the current density the shape of the grains is changing. The deposits obtained with agitation display morphologically well-shaped crystals, some of them elongated with the characteristic tetragonal morphology of tin [15]. Additionally, the coatings made with agitation, present larger crystals and in most of the cases they show coalescence. The tin grains are much bigger than the copper ones obtained under the same conditions.

3.2. CuSn alloy electrodeposition

3.2.1. Voltammetry studies

Two types of electrolytes were proposed for the electrodeposition of the CuSn alloy (Table 5.4).

Table 5.4: Bath composition for the CuSn alloy

Bath I	**Bath II**
$CuSO_4$	$CuSO_4$
$SnSO_4$	$SnSO_4$
H_2SO_4	H_2SO_4
	HBF_4

Tetrafluoroboric acid (HBF_4) was chosen because it is known to keep the metal ions dissolved in the solution and to ensure a consistent deposition of the CuSn alloy. In order to see in which potential limits the electrodeposition of the two metals occurs, several cathodic sweeps were performed (Fig. 5.12).

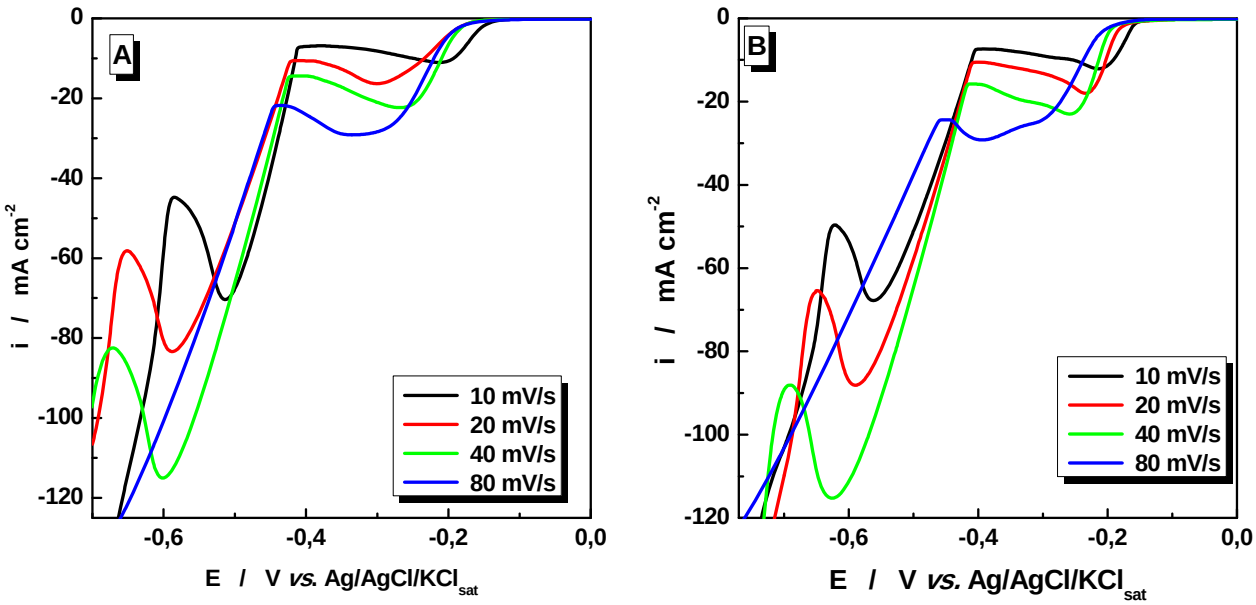

Figure 5.12 Cathodic sweeps of CuSn alloy deposition at different sweep rates recorded at a platinum disc electrode. The electrolyte was prepared at 296 K and contains: (**A**) 0.4M $SnSO_4$ + 0.1 M $CuSO_4$ + 1M H_2SO_4 and (**B**) 0.4M $SnSO_4$ + 0.1M $CuSO_4$ + 0.2M HBF_4 + 1M H_2SO_4

The copper deposition starts in the potential range -0.2 V ÷ -0.4V followed by tin deposition in the potential range -0.45 V ÷ -0.7V. Adding HBF_4 into the bath solution does not significantly change the deposition potentials of the two metals.

3.2.2. Study of copper-tin deposits

3.2.2.1. Deposits obtained by galvanostatic electrolysis

The desired composition for our CuSn alloy study is $Cu_{15}Sn_{85}$. In order to achieve this composition, galvanostatic and potentiostatic measurements were performed. Figure 5.14 presents the SEM images obtained for CuSn deposits, under different galvanostatic conditions from two types of metal containing electrolytes. Information about baths composition is given in Figure caption 5.14.

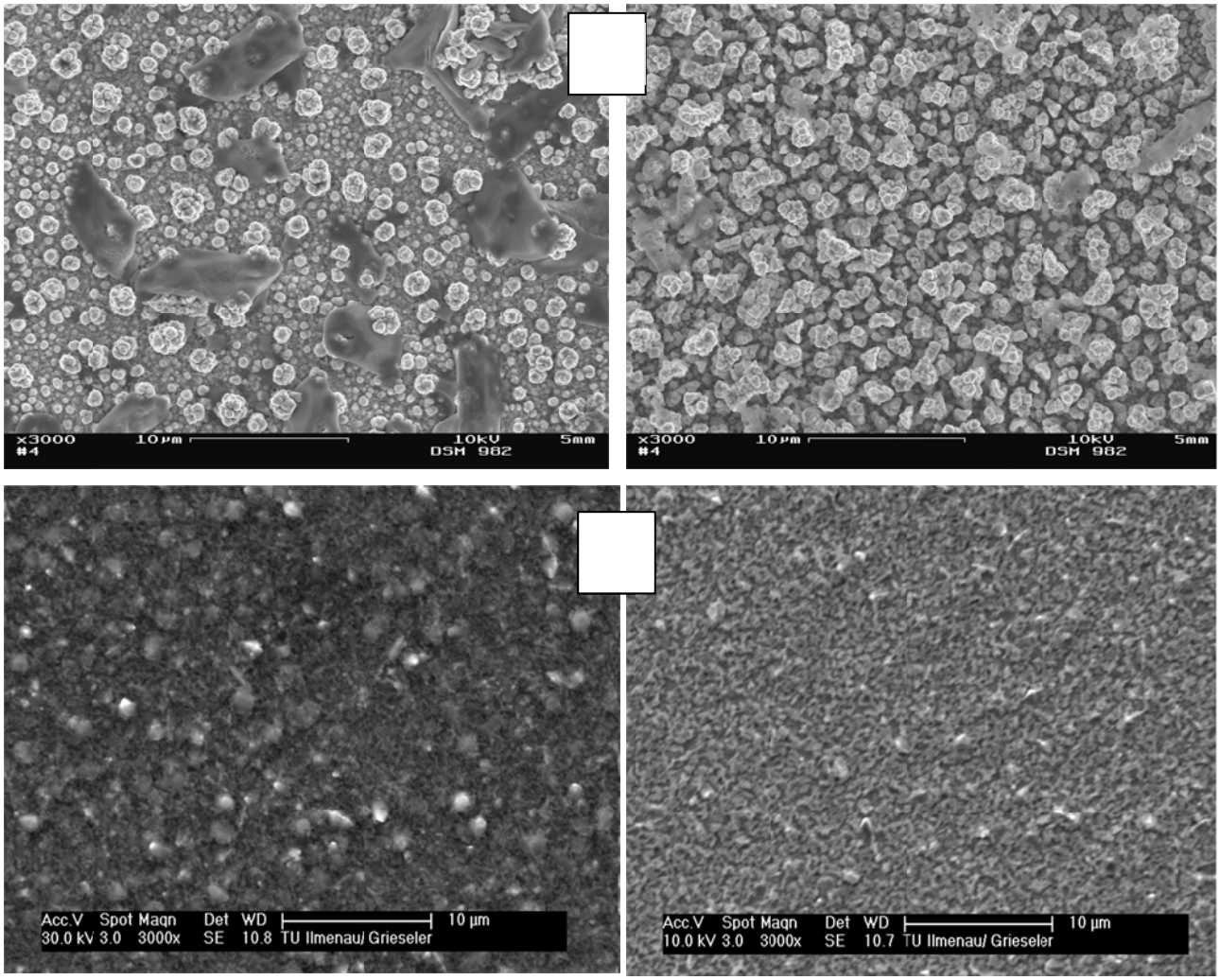

Figure 5.14 SEM micrographs showing the surface morphologies of CuSn films obtained at i = 80 mA/cm^2 (**A**) and i = 120 mA/cm ^{2}(**B**), with stirring (2000 rpm). **Bath I** (0.1 M $CuSO_4$ + 0.4 M $SnSO_4$ + 1 M H_2SO_4) is presented in the left side and **Bath II**(0.1 M $CuSO_4$ + 0.4 M $SnSO_4$ + 1 M H_2SO_4 + 0.2 M HBF_4) in the right side, respectively.

As can be seen in Fig. 5.14, the CuSn alloys have a uniform surface morphology. A small difference between the two baths can be observed: Bath II generates smoother deposits.

3.2.2.2. Deposits obtained by potentiostatic electrolysis

Based on the CV measurements, we obtained CuSn deposits potentiostatically in the range between E = -0.5 V ÷ - 0.7 V. All the potentiostatic deposits had a thickness of 5µm. Information about baths composition is given in Figure caption 5.15.

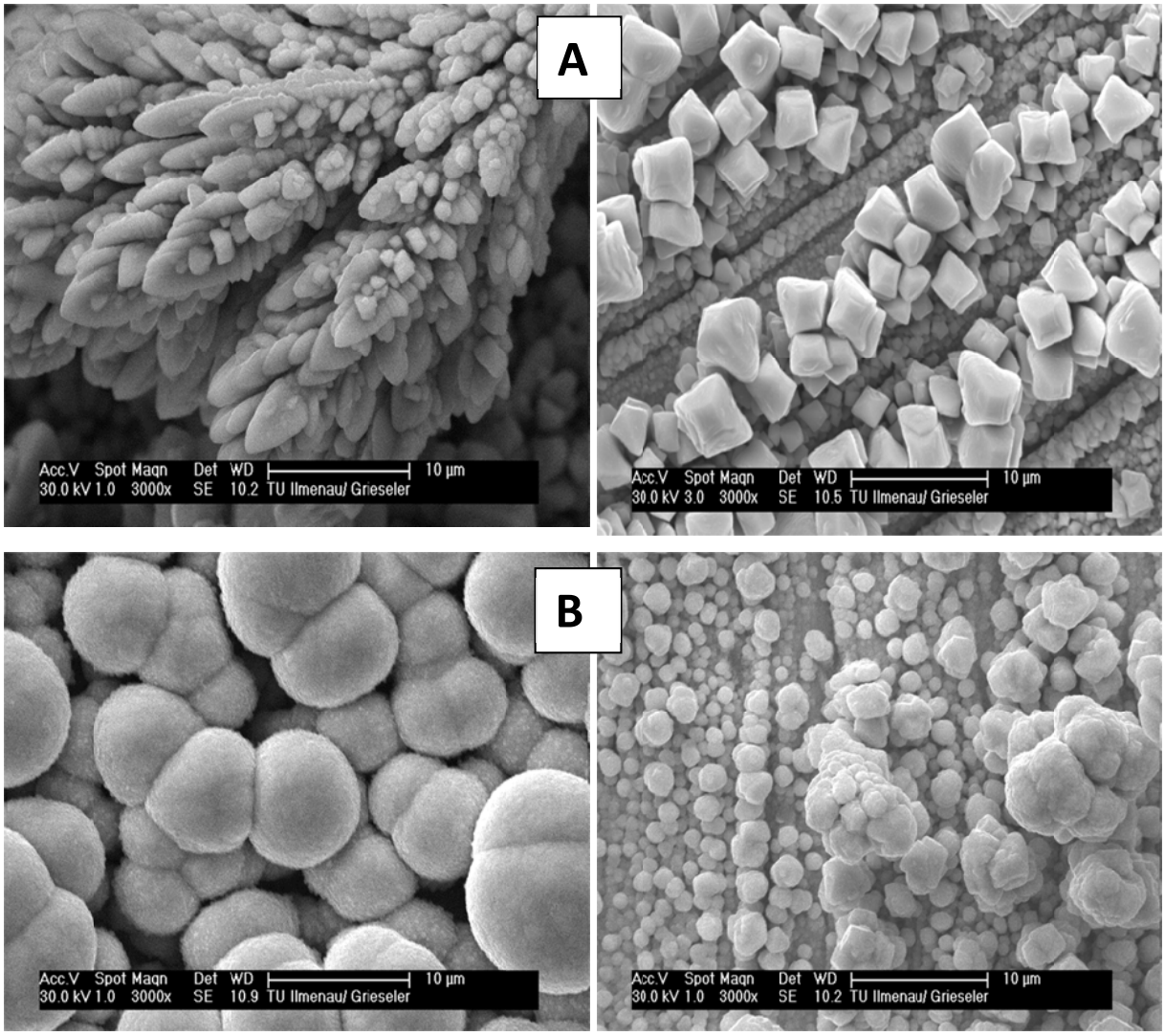

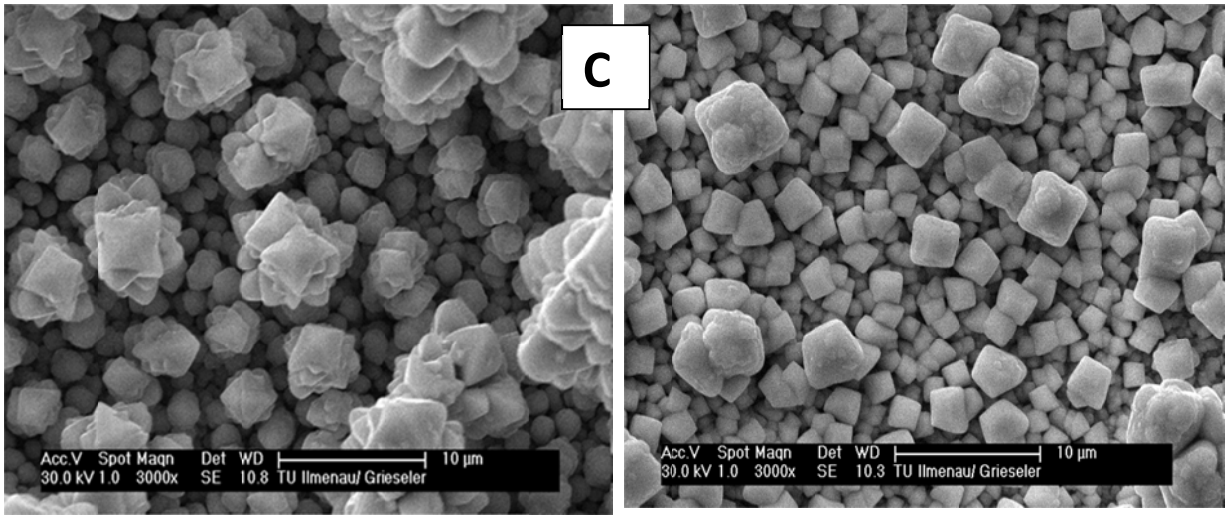

Figure 5.15 SEM micrographs showing the surface morphologies of Cu-Sn films obtained at E = -0.5 V (**A**), E = -0.6 V (**B**) and E = -0.7 V (**C**) with stirring (2000 rpm). **Bath I** (0.1 M $CuSO_4$ + 0.4 M $SnSO_4$ + 1 M H_2SO_4) is presented in the left side and **Bath II** (0.1 M $CuSO_4$ + 0.4 M $SnSO_4$ + 1 M H_2SO_4 + 0.2 M HBF_4) in the right side, respectively.

As it can be seen from Fig. 5.15, for the potentiostatic deposition at E = -0.5 V vs. $Ag/AgCl/KCl_{sat}$ the surface morphology of the deposits looks very sharp and rough. This roughness could be related to the fact that, at E = -0.5V, the deposition of tin just starts. This assumption is in correlation with the CV studies. As the potential increases (see E = -0.6 V and E = -0.7 V) uniform and dense deposits are obtained. Analyzing the insets, we can conclude that the deposits do not present any major differences. The CuSn grains are very small, indicating that the alloy electroplating resulting in a uniform surface morphology.

3.3. EDX analysis

The relation between the metal ratio in the electrolyte is one of the most important relations in alloy deposition. EDX analysis permits us to establish the correlation between the bath and alloy composition.

Table 5.5: Correlation between current density and copper and tin content for deposits obtained from the two types of baths **Bath I** and **Bath II**, the estimated thickness of the deposits was 5 μm.

i	**Cu**	**Sn**
(mA/cm^2)	(wt %)	
Bath I 0.1 M $CuSO_4$ + 0.4 M $SnSO_4$ + 1 M H_2SO_4		
80	65	35
120	48	52
Bath II 0.1 M $CuSO_4$ + 0.4 M $SnSO_4$ + 1 M H_2SO_4 + 0.2 M HBF_4		
80	56	44
120	43	57

Analyzing the alloy deposits obtained under galvanostatic conditions (Table 5.5), we observed that by increasing the current density, in bath I, the Cu content decreased and the Sn content of the deposit increased. Our results are in agreement with the one obtained by Bennett [16]. On the other hand analyzing the alloy deposits, obtained under galvanostatic conditions, when using a bath containing HBF_4 we observed that with increasing current density the Sn content increased. Therefore, in this stage we can conclude that the increase of the current density induces more efficient tin deposition.

EDX analyses were carried out also for the deposits obtained by potentiostatic deposition. Table 5.6 illustrates the composition of the alloys.

Table 5.6: Correlation between potential and CuSn content for deposits obtained from the two types of baths: **Bath I** and **Bath II**, the estimated thickness of the deposits was 5 μm.

E	**Cu**	**Sn**
(V vs. Ag/AgCl)	(wt %)	
Bath I 0.1 M $CuSO_4$ + 0.4 M $SnSO_4$ + 1 M H_2SO_4		
-0.5	87	13
-0.6	58	42
-0.7	61	39
Bath II 0.1 M $CuSO_4$ + 0.4 M $SnSO_4$ + 1 M H_2SO_4 + 0.2 M HBF_4		
-0.5	85	15
-0.6	55	45
-0.7	57	43

At E = -0.5V, in both plating baths, the content of Sn is very small (Table 5.5). This is in good agreement with the galvanostatic and voltammetric results, showing that at this potential the Sn electrodeposition just starts. It can be seen that the positive shift of the potential increases the Sn content in the alloy.

In order to achieve the alloy composition described above, we increased the tin concentration in the electrolyte. Now, the baths have the following composition: 0.1 M $CuSO_4$ + 0.8 M $SnSO_4$ + 1 M H_2SO_4 (**Bath Ia**) and 0.1 M $CuSO_4$ + 0.8 M $SnSO_4$ + 1 M H_2SO_4 + 0.2 M HBF_4 (**Bath IIb**). When potentiostatic mode was used, the experiments were performed for the Cu:Sn ratio = 1:8.

Table 5.7: Correlation between potential and CuSn content for deposits obtained from two types of baths **Bath Ia** and **Bath IIb;** the estimated thickness of deposits was 5 μm.

E	**Cu**	**Sn**
(V vs. Ag/AgCl)	(wt %)	
Bath Ia 0.1 M $CuSO_4$ + 0.8 M $SnSO_4$ + 1 M H_2SO_4		
-0.5	49	21
-0.6	33	67
-0.7	36	64
Bath IIb 0.1 M $CuSO_4$ + 0.8 M $SnSO_4$ + 1 M H_2SO_4 + 0.2 M HBF_4		
-0.5	42	58
-0.6	27	73
-0.7	29	71

The results from EDX analysis are in a good correlation with the concentration changes in the electrolyte composition. The tin content was direct proportional to the potential increase. The highest tin percentage in the deposit (73%) was obtained at E = -0.6V, with bath IIb [17]. The EDX analyses (see Table 5.7) are in good correlation with the surface morphology of the alloy coatings (see Fig. 5.15). As a conclusion, an electrode material with high Sn content was obtained. Alloys with high Sn content have high electrocatalytic activity [4] and the CuSn alloy has the ability to control the ERN to nitrogen gas as final product [9]. Thus, we conclude that the deposit $Cu_{27}Sn_{73}$ is a suitable material for nitrate reduction due to its composition. This material will be investigated further in the electrochemical reduction process (see Chapter 4 and 5).

4. ELECTROACTIVE SPECIES DETECTION RESULTING FROM ELECTROCHEMICAL REDUCTION OF NITRATE AT Cu AND CuSn ALLOYS

After synthesis and characterization of copper, tin and copper-tin alloy, the copper and copper-tin electrode materials were chosen to be used as cathode materials for reduction of nitrate from model nitrate solutions.

The objective in this part of the thesis is the detection of the electroactive species resulting from electrochemical reduction of nitrate (ERN). A simple and fast electrocatalytical methodology for determination of electroactive products resulting from nitrate reduction at a Cu and CuSn electrode in an alkaline media is proposed on the basis of cyclic hydrodynamic voltammetry (CHV) and square wave voltammetry (SWV). In our studies a modified CHV method [18] and a SWV [19] was used for the detection of electroactive products resulting from ERN. The results of SWV were compared with those obtained through CHV. The main purpose in this study was to obtain a fast and cheap analytical method for the electroactive products resulting from nitrate reduction.

The electrochemical measurements were carried out at relative high scan rates (500 mV/s) using a Pt/Cu and a Pt/Cu-Sn RRDE. Cyclic voltammetry combines the high scan rate with the controlled hydrodynamic mass transport. The SWV measurements were performed using the Pt ring as working electrode. After the polishing of the ring-disk electrodes, they were pre-treated by repeated cycling between hydrogen and oxygen evolution regions: -1.5 and +2.0 V vs. $Ag/AgCl/KCl_{sat}$. After the pre-treatment, reproducible current-voltage curves were obtained. For each studied species, the electrochemical cell was first filled with 100 mL of 1M Na_2SO_4 as supporting electrolyte. After that, different amounts of NO_2^-, NH_2OH and NH_4^+ solutions were added successively (resulting concentrations of 0.1, 0.5, 1.0, 2.0 g/L) and the pH was adjusted to 11.0 using 1M NaOH.

4.1. Electroactive species detection in mono-component solutions

In order to evaluate the possibility of electrochemical detection of some electroactive products resulted from ERN in alkaline media, we performed preliminary studies in mono-component solutions using the standard addition method.

Figures 6.1A and 6.1B show the cyclic and square wave voltammograms recorded at the Pt ring electrode in 1 M Na_2SO_4 in the presence of different concentrations of NO_2^-. For clarity, the figures present only the positive potential ranges from the corresponding anodic

scan. The measurements were performed with the disk electrode disconnected; the detection of the individual species was carried out at the Pt ring electrode. In mono-component solutions, well defined oxidation peaks of nitrite (see Fig.6.1) were recorded using both techniques.

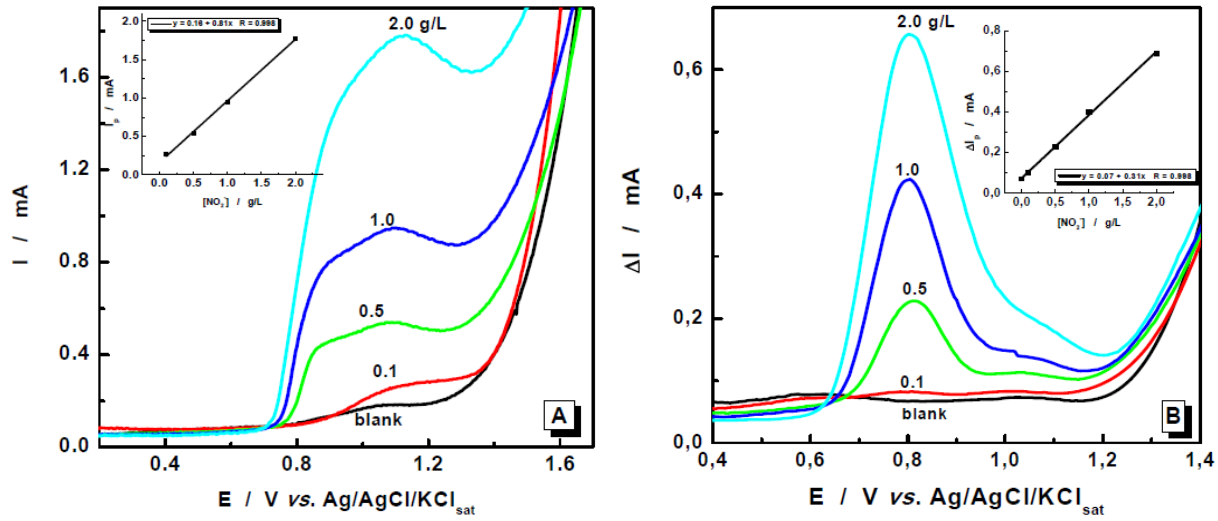

Figure 6.1 Anodic peak current dependence on the NO_2^- concentration by CHV (A) and SWV (B) Experimental conditions: Start potential = -1.5 V and end potential = 2.0 V, ω = 1000 rpm, disk electrode disconnected; CHV: v = 500 mV s^{-1}; SWV: wave amplitude = 50 mV; wave period = 10 ms; wave increment = 5 mV.

As it can be seen in Figure 6.1A, using CHV, the oxidation peaks of nitrite were detected close to + 1.1 V. In SWV (Figure 6.1B) experiments the oxidation peaks for nitrite can be observed at +0.8 V. The SWV measurements reveal well defined peaks and their potential does not vary with the concentration. The insets in Fig. 6.1A and 6.1B show the relationship between the peak current and the nitrite concentration. In both cases a good linear correlation (R = 0.998) can be observed.

Comparing the results obtained previously [20] and SWV for the nitrite oxidation, a ~ 300 mV difference between the peak potential values can be noted. This can be explained by the very poor reversibility of the nitrite oxidation process at Pt and also by the extremely large range of mixed control (kinetic and mass transport, resulting from the combination of the fast potential scan rate and the forced convection). Both factors are inducing a positive shift of oxidation peak potential recorded by CHV. Contrarily, in SWV, where roughly speaking the recorded curves can be considered, as the first order derivate of the cyclic voltammetric records, the observed peak potentials become closer to the equilibrium potential and also the influence of the mass transport is significantly reduced.

The electro-oxidation of nitrite at a Pt electrode was explained by the group of Piela *et* al. [21], where they observed that the nitrite electro-oxidation process strongly depends on the state of the electrode surface. The reaction is inhibited by the oxide layers formed at the platinum electrode surface.

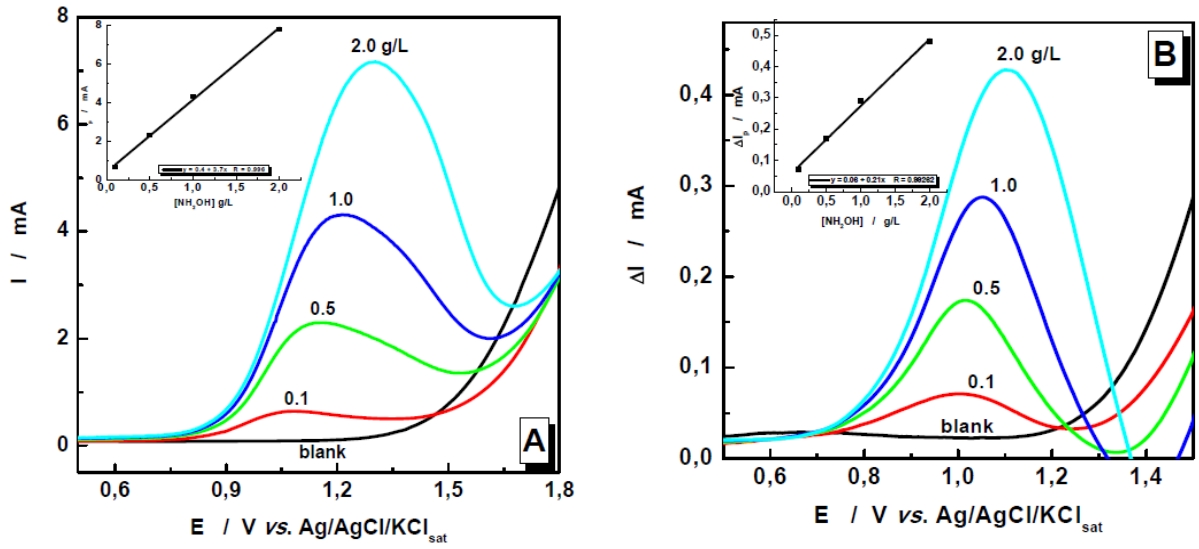

Figure 6.2 Anodic peak currents dependence with NH_2OH concentration by CHV (A) and SWV (B) at a Pt ring electrode.

Figures 6.2A and 6.2B show CHV and SWV data for different concentrations of hydroxylamine and in the inset the relationship between the recorded peak currents and the hydroxylamine concentrations is presented. It is worth noting that for both techniques, a good linear correlation (R= 0.996) between the oxidation peak currents and the hydroxylamine concentration was obtained. In mono-component solutions, depending on the concentration, the oxidation peak potential of hydroxylamine was between +1.1 and +1.3 V for CHV and between +1.0 and +1.1 V for SWV, respectively. Compared to the nitrite oxidation, we observed only a relatively small difference (from 100 to 200 mV) between the peak potentials values measured by CHV and SWV. Taking into account that, the hydroxylamine oxidation process is faster at the Pt electrode, the decrease of this difference sustains the statement mentioned above.

A comparison between Fig. 6.1 and 6.2, when CHV method is used, was reported in [22]. Gadde and Bruckenstein [23] studied the electro-oxidation of nitrite in 0.1M $HClO_4$ at a Pt electrode. Using the RRDE technique, they showed that nitrite reduction is a convective-diffusion controlled process. On the other hand, their product analysis data indicate possible kinetic complications in the electrode reaction because of multiple product formation.

Furthermore, Piela et al. [24] investigated the hydroxylamine oxidation in acidic media at the rotating platinum electrode. They showed that, the reaction kinetic is hindered by the platinum oxide layer formation at the electrode surface. The process is hindered by the oxide, because the reaction was sensitive to all experimental conditions that influence the oxide formation process, *i.e.*, potential, time, and pH.

Anodic sweeps recorded in the presence of different concentrations of ammonium are presented in Figure 6.3.

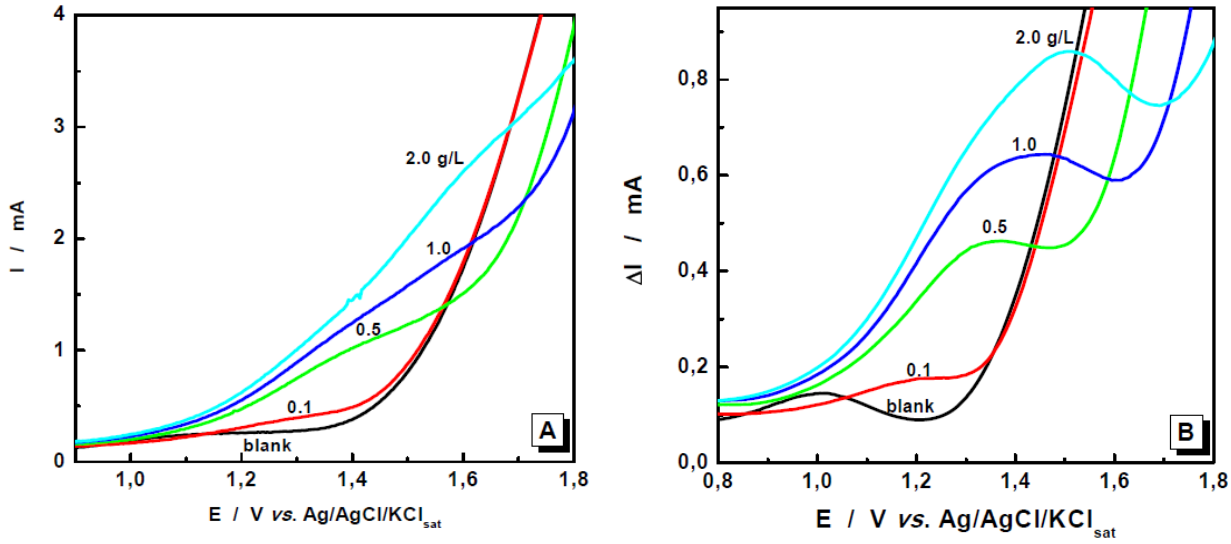

Figure 6.3 Anodic peak current dependence with NH_4^+ concentration by CHV (A) and SWV (B) at Pt ring electrode.

As a result of the fact that at pH = 11 the ratio between NH_3 and NH_4^+ concentrations is 40 [25], ammonium can be electrochemically detected by ammonia oxidation (see Fig.6.3.). The CHV measurements for different concentrations of ammonium reveal only poorly defined plateaus at ring potentials higher than +1.3 V. On the other hand, SWV measurements revealed well defined peaks for ammonia oxidation at ring potentials between +1.2 and +1.5 V, demonstrating that the SWV based method is more suitable for electrochemical detection of ammonia than CHV.

Due to the high sensitivity and the rejection of background currents, SWV can be successfully used for the individual detection of all the three involved species. Three different peak potentials were attributed: + 0.8 V for NO_2^- oxidation, +1.0 V for NH_2OH oxidation and approximately +1.3 V for ammonia oxidation.

4.2. Electrocatalytic stability of the electrode material

In order to evaluate the possibility of simultaneous electrochemical detection of electroactive products resulting from ERN in alkaline media, a working disk electrode of Cu or CuSn was used. This choice was based on the fact that this material has a well-known electrocatalytic activity for ERN and depending on the electrolyte composition and applied potential, a wide variety of species can be generated. For each set of measurements, the working disk electrode (Pt covered with Cu or CuSn) was polarised at a constant potential. Potentiohydrodynamic measurements were performed at the Pt ring electrode (between -1.5 and +2.0 V) and eight successive cycles were recorded without refreshing the Cu or CuSn layer.

For an accurate comparison, before each set of CHV and SWV measurements, the surface of the Pt disk electrode was covered with a thin layer (5 μm) of freshly electrodeposited Cu or CuSn. The experimental conditions for obtaining the electrode materials were presented in the previous section (see Chapter 3). The anodic currents recorded at the Pt ring electrode, corresponding to the oxidation of species generated at the disk, were analysed. Figure 6.5 presents three examples of the currents recorded by SWV at the Pt ring electrode during the anodic scans, for different disk polarisation potentials. Only the anodic parts from the 1st, 2nd, 4th and 8th cycle, at a Cu electrode are presented in Figure 6.5. Depending on the applied potential of the Cu and CuSn disk electrode, currents corresponding to different electroactive species were recorded.

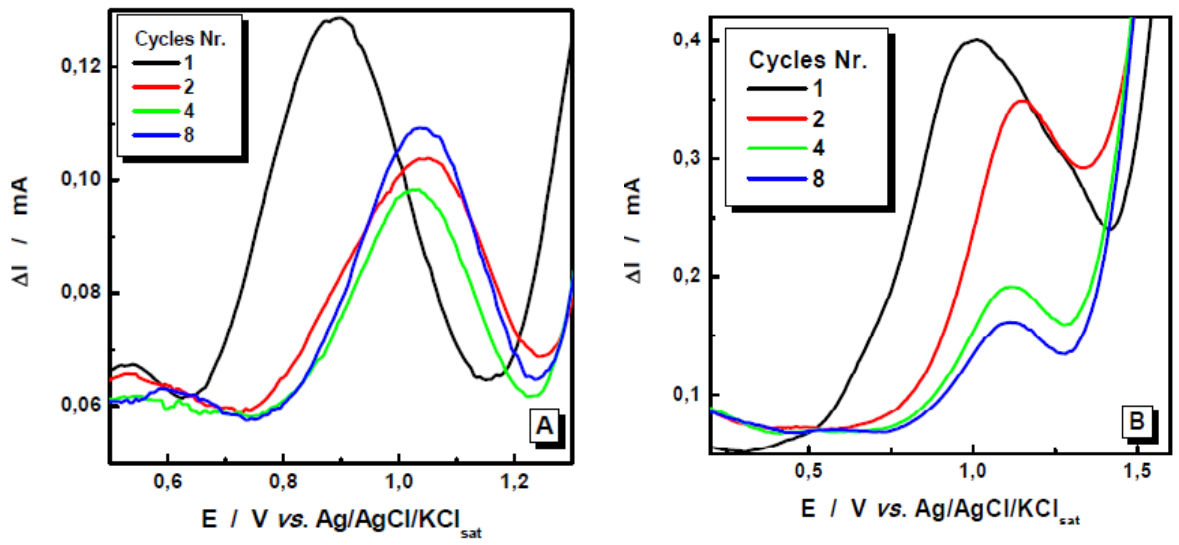

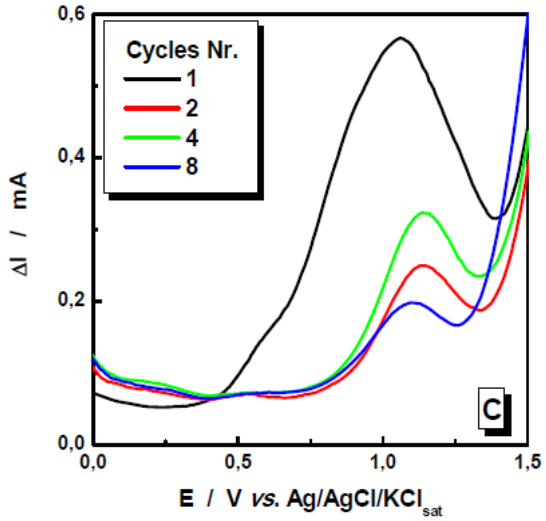

Figure 6.5 Current evolution on the Pt ring electrode at different Cu disk potentials: (**A**) -0.9 V, (**B**) - 1.3 V and (**C**) – 1.7 V in 2 g/L NO_3^- solution containing 1 M Na_2SO_4 (pH = 11) as supporting electrolyte.

Figure 6.6 presents voltammetric currents recorded at the Pt ring electrode during the anodic scans for two different disk polarization potentials. Measurements were performed by measuring eight successive cycles without CuSn layer refreshing.

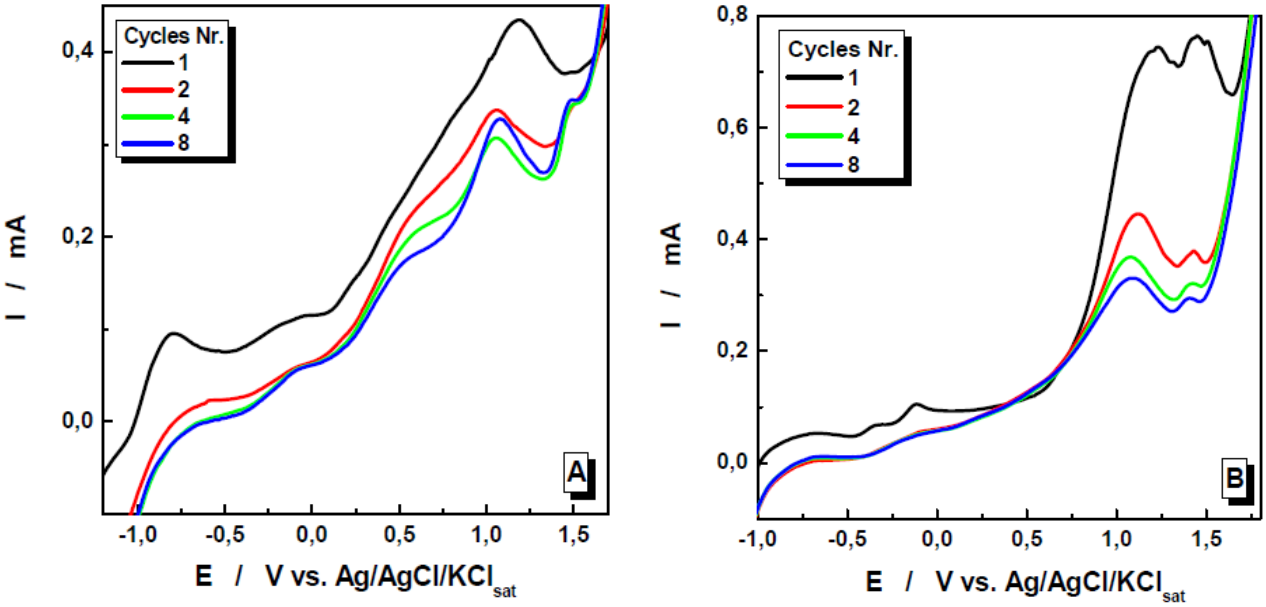

Figure 6.6 Current evolution on the Pt ring electrode at different CuSn disk potentials: (**A**) -1.0 V and (**B**) - 1.5 V in 2 g/L NO_3^- solution containing 1 M Na_2SO_4 (pH = 11) as supporting electrolyte.

It can be observed that for the selected potential range, every first cycle indicates a maximum electrocatalytic activity, which decrease rapidly in the following sweeps. Moreover, it can be observed that, after the first cycle, the peak potentials corresponding to the currents recorded at the Pt ring electrode are shifted to more positive values, suggesting a blocking of the surface. The decrease of the copper electrode electroactivity after the first

cycle may be related to the adsorption of hydrogen and nitrate reduction products [26, 27, 28]. Reyter et al. [6] studied in detail the electrocatalytic activity of the copper electrode and reached the conclusion that the "deactivation" of the copper electrode observed during the first stage of the electrolysis may be related to the adsorption of N-containing species, limiting further nitrate reduction. As a solution, they propose a reactivation of the electrode by a periodic application of a square wave potential pulse of -0.5 V in order to desorb the poisoning species.

4.3. Simultaneous detection of electroactive products

4.3.1. Simultaneous detection in mixed solution

In order to test the simultaneous detection of the electroactive products resulting from nitrate reduction, a new experimental set similarly to CHV was performed. The experiments were carried out in mixed solutions, containing different concentrations of NO_2^-, NH_2-OH and NH_4^+. An initial concentration of 0.5 g/L $NO_2^-$was used, followed by 0.2 g/L NH_2OH and 0.5 g/L NH_4^+. The obtained results showed that the involved species interact, making their individual detection difficult (Fig. 6.10).

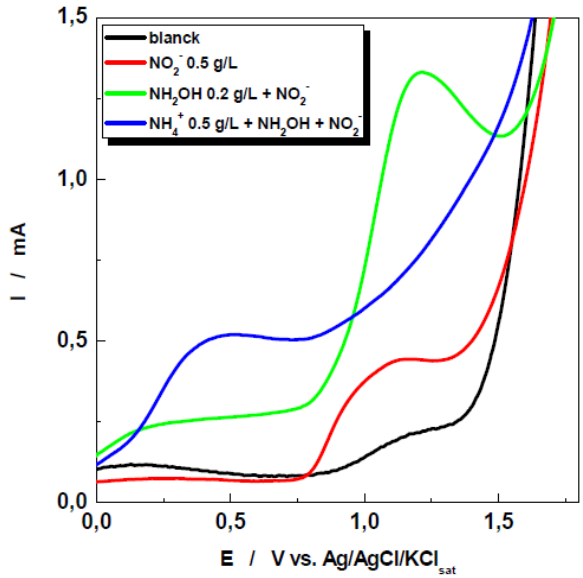

Figure 6.10 CHV in a mixed solution of NO_2^-, NH_2OH and NH_4^+ species at a Pt ring electrode.

Horyani *et al.* [29] studied the electrocatalytic reduction of nitrates in mixed solutions at a platinum electrode in alkaline media and concluded that in a system containing NO_2^- and NH_3 a mixed process occurs; this can be attributed to the adsorption competition between reacting species and the other components present in the system, or formed under the experimental

conditions. We should note here that, the investigation on the reaction kinetics and mechanism is not an objective in the current work.

4.3.2. Simultaneous "in situ"detection of generated electroactive species at a Cu and CuSn electrodes

Based on the above discussed results and by reactivating the surface of the Cu and the CuSn electrode before each experiment, we started a detailed study concerning the influence of the polarization potential of the electrode on the ERN product composition. As shown in Fig. 6.11, the decrease of the disk potential to more negative potentials causes an increase in the recorded ring currents. Depending on the disk potential, the currents recorded on the ring electrode correspond to the oxidation of different intermediate or final products of nitrate reduction.

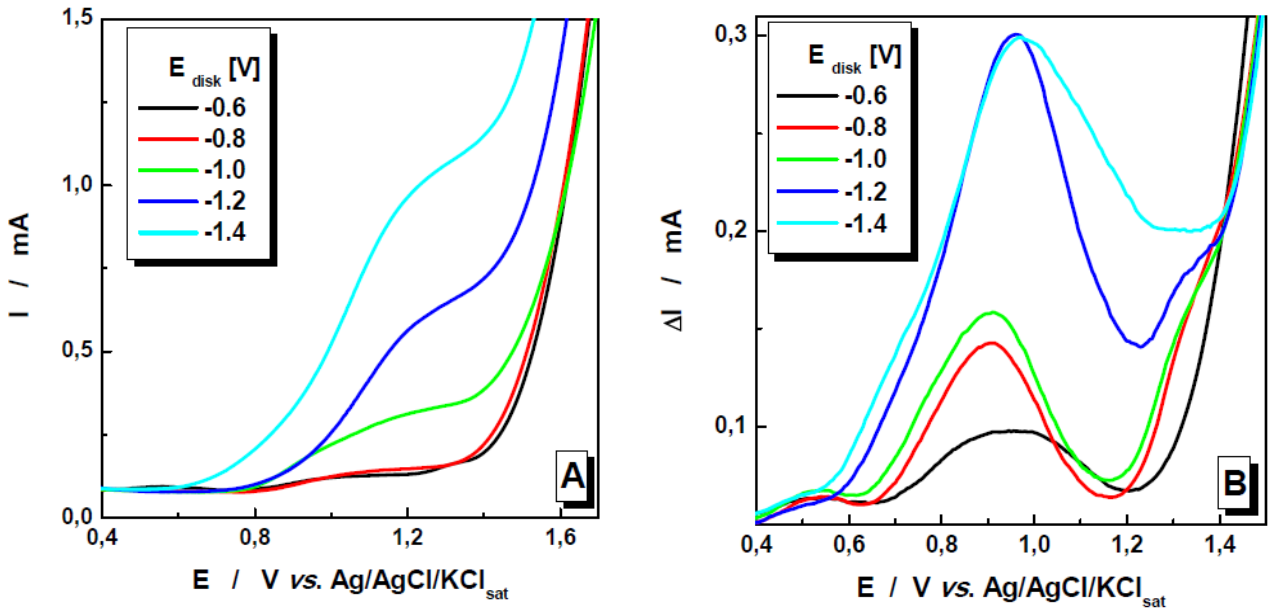

Figure 6.11 Influence of the polarization potential of the Cu disk surface on the oxidation currents recorded by CHV (A) and SWV (B). Experimental conditions: start potential = -1.5 V and end potential = 2.0 V, ω = 1000 rpm, wave amplitude = 50 mV; wave period = 10 ms; wave increment = 5 mV. The Cu plated disk electrode was polarised at different constant potentials as indicated in the legends.

As discussed in the theoretical part of this study, NH_3 is one of the final products that are mainly obtained when a copper disk electrode is used. Therefore, for a better evaluation of the ERN pathway, the disk electrode was polarized at constant potential values between -0.6 V to -1.4 V with a 0.1 V increment. As can be seen from Fig. 6.11A, by using CHV, only a poorly

defined oxidation plateau can be observed for ring potentials between + 1.0 V and + 1.4 V [30]. On the other hand, SWV measurements (see Fig. 6.11B) reveal two different oxidation processes. The voltammograms show that the SWV detection gave a well-defined anodic wave with a peak potential of 0.9 V in alkaline media. Based on the results obtained in mono-component solutions, the first anodic peak (positioned around 0.9 V) can be associated to nitrite and/or hydroxylamine oxidation. The oxidation peak of nitrite in mono-component solution has the maximum at 0.8 V and hydroxylamine at 1.0 V. A possible explanation for the peak displacement could be the two simultaneous oxidation processes (NO_2^- and NH_2OH) that are taking place. Due to the latter reason, that the hydroxylamine oxidation process is faster than of nitrite, the oxidation current of hydroxylamine overlaps partially the oxidation current of $NO_2^-$and as result the peak is shifted towards more positive values.

For disk potentials more negative than -0.8 V, a clear signal corresponding to ammonia oxidation, can be observed at ring potentials starting at 1.3 V. Since the ammonia oxidation peak is better defined and sufficiently separated from the oxygen evolution peak, it was possible to confirm the presence of ammonium between the ERN products.

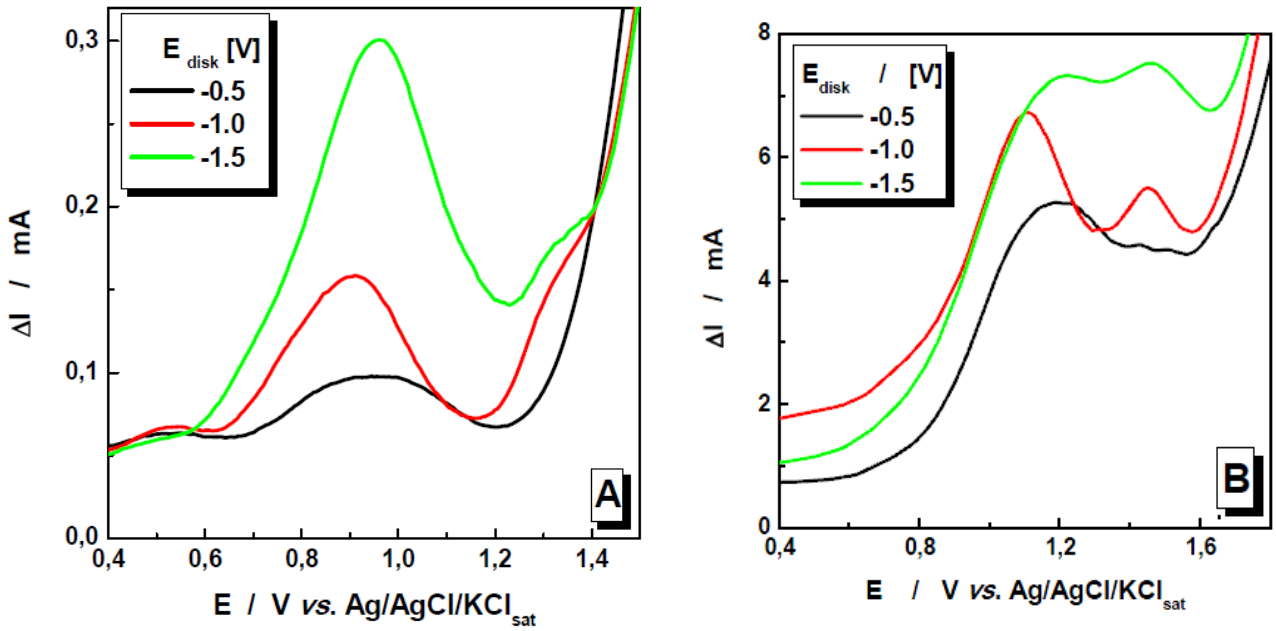

Figure 6.12 Influence of the polarization potential on the oxidation currents recorded by SWV at a Cu (A) and CuSn (B) disk electrode. Experimental conditions as in Figure 6.11.

In the case of the CuSn electrode (Fig. 6.12), the electrocatalytic activity of the electrode material is improved. Two distinct current peaks are observed. Based on the results obtained in mono-component solutions, the first one (~ 1.0V) can be attributed to nitrite (see Fig. 6.1) and hydroxylamine (see Fig. 6.2) oxidation. For disk potentials more negative than -0.5V, a

clear current response, corresponding to ammonia oxidation, can be observed at ring potentials starting at 1.3 V. In comparison with the Cu electrode, the CuSn electrode displays an improved electrochemical activity [31].

Bouzek *et al*. [32] and Gootzen *et al*. [33] reached the conclusions that, from all possible products that are formed during the nitrate reduction only nitrite and hydroxylamine are sensitive towards oxidation at the platinum ring electrode and other possible products like NH_4^+, N_2 and N_2O are not susceptible towards oxidation at the platinum ring electrode. Contrarily, Endo *et al.* [34] studied the oxidation of ammonia on a disk electrode and concluded from RRDE experiments that, two kinds of intermediates involved in the anodic oxidation of ammonia on platinum could be detected in situ; one can then be reduced (probably NO_x) and another can be further oxidized (such as NH_2OH).

In our experimental conditions, the possibility of electrochemical detection of ammonia via the ammonia oxidation at a Pt ring electrode was demonstrated. From the above discussion it was shown that, at least three electroactive products resulting from ERN at a copper plated Pt electrode in alkaline media can be detected by the SWV technique. The difference between the results obtained by the SWV and CHV were found to be significant, proving the superiority of the SWV based method. Comparing the two techniques, it is worth to note that, if the electrochemical processes have reasonable differences between the characteristic potentials, only SWV allows accurate evaluation of peak potentials and currents. Moreover, using the cyclic SWV for the detection of the resulting products we can obtain a more detailed picture of the global electrochemical process that takes place at the disk electrode. The results obtained with CHV and SWV allow a fast in situ analysis of the electrocatalytic properties of the electrode materials, proving the possibility of quantitative evaluation of individual electroactive species. In comparison to pure Cu electrode material, an enhancement of the electrocatalytic activity of Cu by alloying with Sn was observed. The optimal conditions for the voltammetric detection of electroactive species resulting from nitrate reduction were established, which provides useful information for the optimization of the ERN process.

5. DIRECT REDUCTION IN AN ELECTROCHEMICAL FLOW REACTOR
5.1. Design of the electrochemical reactor

An electrochemical flow reactor, as presented in Fig. 7.1, was used for the electroreduction of nitrates. The cell was operated in a divided configuration, to remove possible interferences such as nitrite oxidation at the anode. A model electrolyte ($NaNO_3$, NaOH) was used in the cathodic compartment. In both compartments, a volume of 300 mL of solution was recirculated. The anolyte was 1.0 M NaOH. Constant current electrolysis tests were performed using various cathode materials. The cathode and anode chambers were separated by a Nafion® 324 (DuPont) cation selective – membrane (separator). The investigated cathode materials were copper (Cu) and a copper-tin alloy (CuSn). An oxygen evolving dimensionally stable anode (DSA) was used. The anodic and cathodic compartments were of equal volume (10 mL). The tightness of the cell was achieved by using rubber frames, specially designed for the reactor. The geometrical area of the cathode and the anode was 10 cm^2 and the distance between the two electrodes was 1 cm. The flow cell design is shown schematically in Figure 7.2. The electrolytes were recirculated through the cells compartments with a double channel peristaltic pump, having a monitored flow rate. In order to analyse the nitrate and nitrite concentration, at specific time intervals, samples were withdrawn from the cathode compartment by using a syringe and were analyzed, after the appropriate dilution. The determination of nitrate and nitrite was performed by ion chromatography (Dionex DX 100 with an anion column for AG 14A/AS14 A) (see Chapter 4.1.7).

Figure 7.1 Electrochemical flow reactor for nitrate removal

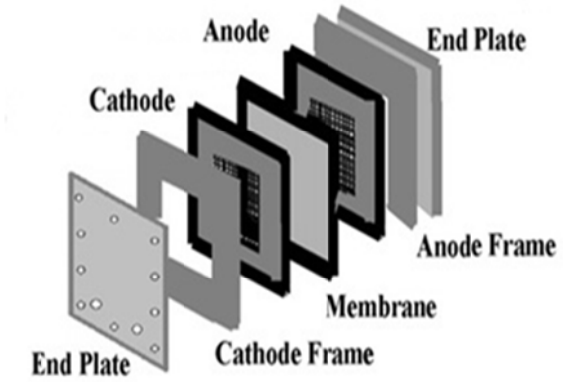

Figure 7.2 Schema of the electrochemical flow reactor

5.2. Effect of applied current density and flow rate on the ERN

In order to investigate the nitrate reduction process, prolonged electrolyses were carried out at different current densities. In the electrochemical reduction process, the nitrate removal rate is proportional to the concentration of nitrate and to the hydrogen concentration. The kinetic equation for nitrate removal is [35]:

$$\frac{-d[NO_3^-]}{dt} = k[NO_3^-] \qquad (7.6)$$

The apparent rate constant was studied for reduction process by plotting log $[C_i/C_t]$ vs. time, where C_t is the concentration of nitrate at time t and C_i is the initial nitrate concentration. The plot gives a straight line which indicates that it follows a pseudo first order kinetics [35]. From the slope of equation:

$$\log_{10}[C_t/C_i] = -kt/2.303 \qquad (7.7)$$

the apparent rate constant, k, was calculated.

Based on the voltammetric analysis (see Fig. 7.3), galvanostatic electrolysis experiments were performed at three current densities at a Cu and CuSn cathode. Moreover, the influence of the flow rate on the electrochemical reduction of nitrate was investigated.

Figure 7.4 displays the evolution of the nitrate and nitrite concentration during prolonged electrolyses at different flow rates at: (A) 10 mA cm^{-2} and (B) 5 mA cm^{-2} cathodic current densities.

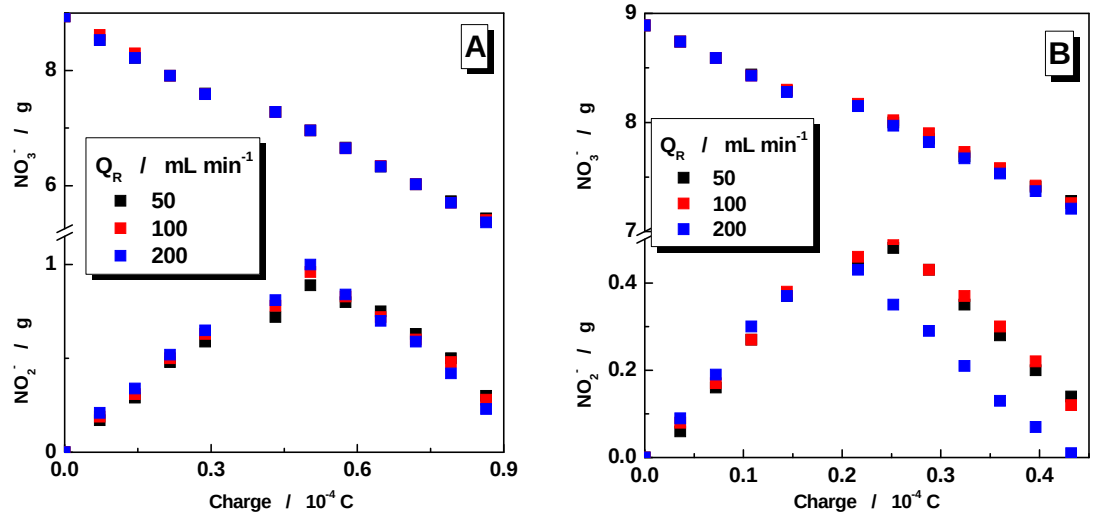

Figure 7.4 Evolution of the concentration of NO_3^- and NO_2^- *vs* charge. Experimental conditions: 0.1M $NaNO_3$ in 1M NaOH electrolyte solution; (A) -10 mA cm^{-2} at a Cu electrode and (B) -5 mA cm^{-2} at a CuSn electrode

The concentration of nitrite initially increases, reaches a maximum and consequently decreases (Fig. 7.4). The form of this curve is characteristic for an intermediate product generated in a consecutive reaction mechanism:

$$NO_3^- \rightarrow NO_2^- \rightarrow Products \qquad (7.8)$$

This suggests that the conversion of nitrite to other reduction products is the slow step in the reaction mechanism. At CuSn, after a slight increase of nitrite concentration, both nitrite and nitrate decrease throughout the experiment. Overall, Cu and CuSn present the same rate of removal of NO_3^-/NO_2^-. After a period of 24 h of electrolysis a nitrate conversion of 40% was achieved at a Cu cathode (see Fig. 7.4A) and, on the other side, a conversion of 20% is achieved at a CuSn cathode (see Fig. 7.4B). Given that the current density used in the case of Cu electrode is two times higher than on CuSn electrode, the conversion proportionality observed in our experiments comes to sustain the above results. On the other hand, it can be seen that, at these low current densities, the flow rates have a minimal influence on the reduction process (Fig. 7.4).

The apparent rate constant (k) of the reaction was calculated (Fig. 7.5) based on pseudo first order kinetics described above (Eq. 7.7). The mean k values were ≈ 3.3 min^{-1} for Cu and ≈ 1.4 min^{-1} for CuSn, respectively. Moreover, at these low current densities, charge transfer occurs slowly and, therefore, the mass transport does not have influence (Fig. 7.5).

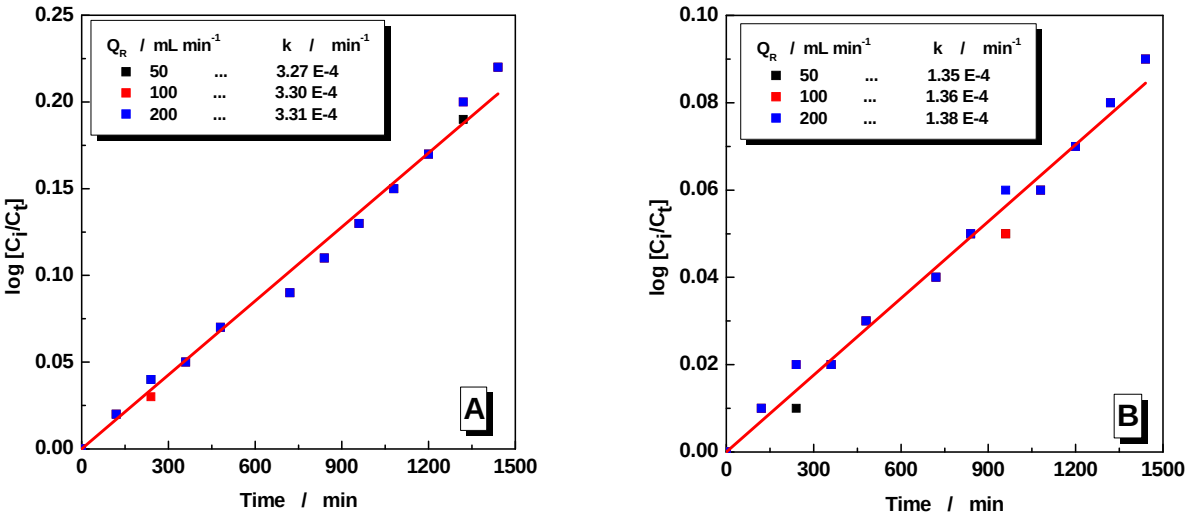

Figure 7.5 Logarithmic representation of nitrate conversion vs. time for apparent rate constant evaluation. Experimental conditions: 0.1M $NaNO_3$ in 1M NaOH electrolyte solution; (A) -10 mA cm^{-2} at a Cu electrode and (B) -5 mA cm^{-2} at a CuSn electrode

Measurements involving prolonged electrolysis were performed at higher current densities: (A) -20 mA cm^{-2} at a Cu electrode and (B) -25 mA cm^{-2} at a CuSn electrode. The experimental data are presented in Figure 7.6.

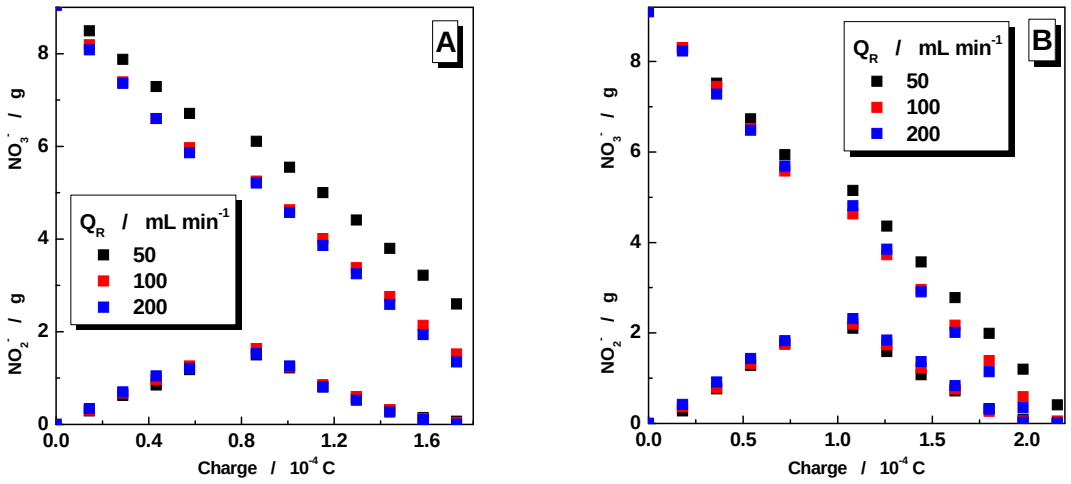

Figure 7.6 Evolution of the concentration of NO_3^- and NO_2^- *vs* charge. Experimental conditions: 0.1M $NaNO_3$ in 1M NaOH electrolyte solution; (A) -20 mA cm^{-2} at a Cu electrode and (B) -25 mA cm^{-2} at a CuSn electrode

As it can be seen, after 24 h of electrolysis, at the Cu cathode the final concentration of nitrate reaches 1 g/L and it is totally eliminated at the CuSn cathode. Given that the current density at the CuSn electrode is higher with 0.05 mA cm^{-2}, the electroreduction of nitrate is more effective at the CuSn electrode. Moreover, the maximum concentration limit (MCL) is at the CuSn electrode achieved.

The nitrite concentration increases at the Cu electrode (Figure 7.6A) and, after that, is further diminished under the MCL after 24 h of electrolysis.

In the case of CuSn electrode (Figure 7.6B), the nitrite content increases and then is successfully removed under MCL. The *k* could not be calculated for the above experimental conditions (see Fig. 7.6) because the reaction does not follow a pseudo first order kinetics (Fig. 7.7). This could be explained by changes that appear in the mechanism of the reaction at these current densities (Fig. 7.6).

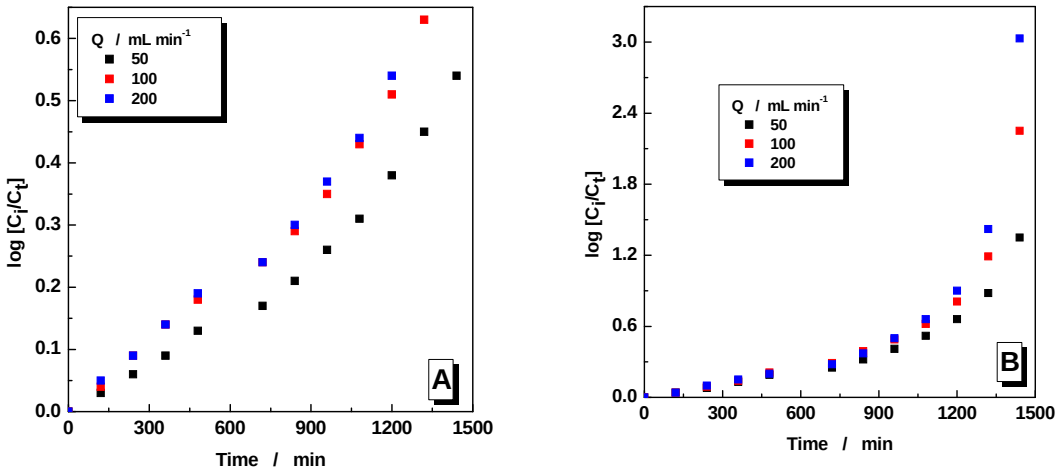

Figure 7.7 Logarithmic representations of nitrate conversion vs. time. Experimental conditions: 0.1M $NaNO_3$ in 1M NaOH electrolyte solution; (A) -20 mA cm^{-2} at a Cu electrode and (B) -25 mA cm^{-2} at a CuSn electrode

Since the mechanism of the reaction changes at the previously studied current densities (Figure 7.6 and 7.7), ERN was further investigated at even higher current densities in order to establish the best working parameters. For this purpose, prolonged electrolyses were carried out at: (A) -40 mA cm^{-2} at a Cu electrode and (B) -50 mA cm^{-2} and CuSn electrode. The data obtained using the same electrolyte, 0.1M $NaNO_3$ in 1M NaOH, are presented in Figure 7.8.

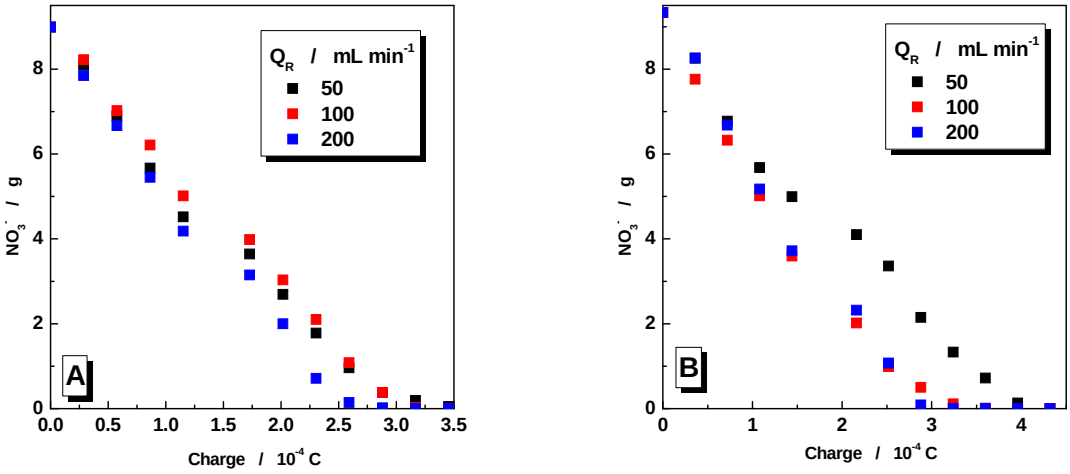

Figure 7.8 Evolution of the concentration of NO_3^- *vs* charge. Experimental conditions: 0.1M $NaNO_3$ in 1M NaOH electrolyte solution; (A) -40 mA cm^{-2} at a Cu electrode and (B) -50 mA cm^{-2} at a CuSn electrode

As it can be seen from Figure 7.8, the conversion of nitrate to a value under MCL (50 mg/L), at Cu and CuSn electrode materials, was achieved. The obtained results show that at the same charge quantity (~ $0.29 \cdot 10^{-4}$ C·cm^{-2}) and flow rate (200 mL·min^{-1}), for the Cu

electrode, a period of 18 h is sufficient to reduce the nitrate under MCL, while for the CuSn electrode, after 14 h the ERN is completed. Thus, we can conclude that at higher current density values, the ERN is more effective at the CuSn electrode.

In this case, the *k* value was not calculated for the above experimental conditions. A more complicated reaction mechanism than the one presented above (see Eq. 7.7) describes the process at high current densities. In this situation, the hydrogen evolution reaction (HER) is intense and the evolved hydrogen participates to nitrates and/or nitrites reduction. Moreover, HER participates by itself to a mass transport enhancement by increasing the turbulence in the closed reactor used for the experiments.

As a conclusion, the experimental measurements showed that, at low current density values, the charge transfer occurs slowly and therefore, the mass transport does not have a noticeable influence on the ERN process. The process follows a pseudo first order kinetics at low current densities, while at high current densities the process follows a more complex mechanism. The HER is intense and the evolved hydrogen participates to nitrates and/or nitrites reduction. Moreover, HER participates by itself to a mass transport enhancement by increasing the turbulence in the closed reactor used for the experiments. Moreover, the prolonged electrolysis performed at high current densities is more efficient if the flow rate is high. Therefore, the MCL of nitrate is achieved in shorter time. The electroreduction of nitrate is more effective at the CuSn electrode.

Contrarily to Prasad et al. [35] and Koparal et al. [36] that come to sustain that higher current densities cannot be used for the treatment of nitrate in order to achieve better treatment efficiency, our results show an opposite effect. Our recent studies prove that higher current densities can be combined with a high flow rate in order to achieve higher conversion efficiency.

5.3. Performances of the electrochemical reactor

The energy consumption for the removal of nitrate and nitrite represents an essential parameter in the evaluation of the process performances. For cost evaluation of the ERN process it is important to identify the most efficient electrode material. Fig. 7.14A and B shows the concentration decay of nitrate at Cu and CuSn electrodes, respectively, obtained at a flow rate of 200 ml min^{-1}, from a solution containing 0.1M $NaNO_3$ in 1M NaOH, at three different current densities.

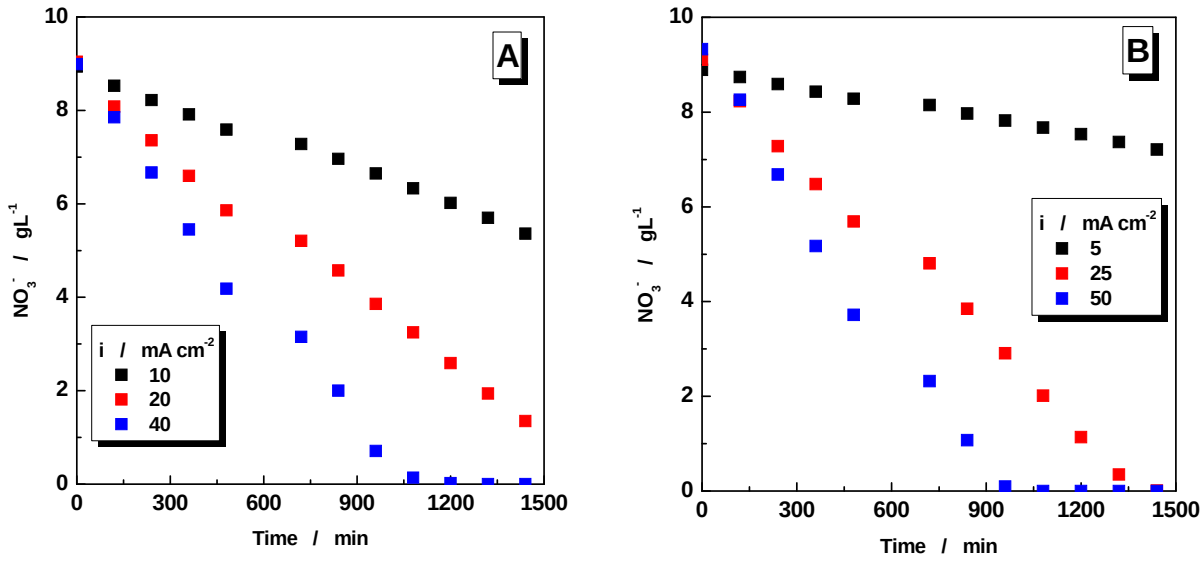

Figure 7.10 Concentration profile of nitrate vs. time at a Cu (A) and CuSn (B) electrode. Experimental conditions: flow rate of 200 mL·min^{-1}; electrolyte: 0.1M $NaNO_3$ + 1M NaOH

In order to reach the MCL, the prolonged electrolyses need to have a conversion degree for nitrate of 99.5%. As it can be seen above (Fig. 7.10) at the Cu electrode the MCL was achieved just at -40 mA·cm^{-2} after 20 h. On the other hand, for the CuSn electrode, at -25 mA·cm^{-2}, the MCL was achieved after 22 h, while at the highest current density (-50 mA·cm^{-2}) the MCL was reached after 18 h.

Based on the experimental results (see Fig. 7.10) it can be stated that the CuSn electrode exhibits a better performance for the ERN process, illustrated by shorter reaction times and lower energy consumption.

The key parameters which describe the ERN process were evaluated based on the experimental results. The data are presented in Table 7.2. The time values from Table 7.2 represent the duration of electrolysis until MCL was reached. All the values were calculated at a flow rate of 200 mL·min^{-1}.

Table 7.2: Current efficiency (r_F) and energy consumption (W_s) values for the ERN at Cu and CuSn electrodes, obtained in synthetic nitrate solutions.

Electrode material	i (mA/cm^2)	E_{cell} (V)	Time (h)	r_F (%)	W_s (kWh/kg $NaNO_3$)
Cu	10	2.9	24*	48	4
	20	4.8	24*	35	9
	40	6.5	20	21	15
CuSn	5	2.4	24*	74	2
	25	2.9	22	34	4
	50	5.5	18	22	16

*the MCL was not reached in the given time period

Based on the energy consumption data (Table 7.2) the following conclusions were formulated:

In the studied current density ranges, for treatment of the same volume of solution, the ERN process needs less energy when a CuSn alloy cathode is used. This could be explained by the higher electrocatalytic activity (see Chapter 4) of the alloy in comparison with the pure metal surface.

The calculated W_s values (at higher current densities) are in accordance with those obtained by Katsouranos et al. [4], who succeeded to remove nitrate from an alkaline medium at an energy consumption of 16.5 kWh/kg $NaNO_3$ at a Sn electrode. Similarly, Reyter et al. [37] studied the electroreduction of nitrate at a Cu electrode and obtained an energy consumption value of 25 kWh/kg $NaNO_3$.

The results for the energy consumption summarized in Table 7.2 depend strongly on the pilot unit configuration and they could be significantly improved by a better design of the electrochemical reactor.

6. GENERAL CONCLUSIONS

The present doctoral thesis was focused on the electrochemical removal of nitrate and nitrite from alkaline model nitrate solutions.

The first part of the thesis is dedicated to literature review. It has been explained that the electrochemical reduction of nitrate (ERN) is useful also at high concentrations of nitrate where the biological methods cannot be applied. By applying the electrochemical methods, nitrates can be reduced to nitrite, hydroxylamine, ammonia, nitrogen oxides and molecular nitrogen; products that strongly depend on the nature of the electrode material.

Chapter 3 deals with the synthesis of the electrode materials (Cu and CuSn alloy) used for ERN. The CV studies allowed us to establish the specific parameters concerning the electrodeposition of the individual metals and their alloy.

SEM images taken for copper, tin and copper-tin alloy deposits indicate significant changes in their surface morphology by modifying the electrodeposition parameters (Fig. 5.10-5.15). Moreover, the RDE experiments showed that the rotational speed (intensified mass transport) plays an important role in the process of electrodeposition.

The EDX analyses confirmed that a CuSn alloy was obtained with a content of 27% Cu and 73 % Sn, respectively ($Cu_{27}Sn_{73}$). This alloy electrode material had the highest content of Sn obtained and based on the literature study it is suitable for nitrate reduction due to its composition.

The electrocatalytic properties of the synthesized electrode materials were further investigated in Chapter 4. For this purpose the detection of the electroactive species resulting from ERN was investigated. A simple and fast electroanalytical methodology for determination of electroactive products resulting from nitrate reduction in an alkaline media is proposed on the basis of cyclic hydrodynamic voltammetry (CHV) and square wave voltammetry (SWV). These methods allowed us to detect simultaneously the involved species resulting from ERN (Fig. 6.12). It was demonstrated that the electroactive products resulting from ERN in alkaline media can be detected by the SWV technique at a Pt electrode. Moreover, using SWV ammonium can be electrochemically detected with good accuracy (no SWV literature data are available up to now concerning ammonium detection).

The measurements performed in mono-component solutions prove that, by combining cyclic and square wave voltammetry at high scan rates with hydrodynamic techniques and using an adequate pH value, at least three different electroactive species generated from the NO_3^- reduction (NO_2^-, NH_2-OH and NH_4^+) can be electrochemically detected.

Using both techniques, the optimal conditions for the voltammetric detection of electroactive species resulting from nitrate reduction were established. The results obtained with the CHV and SWV techniques allow a real-time evaluation of the electrocatalytic properties of the used electrode material.

The electrocatalytic activity of the Cu and CuSn electrodes was investigated in Section 4.3. The voltammograms, recorded successively without Cu layer refreshing, demonstrated that the electrocatalytic activity of the electrode material decreased. This decrease is explained due to the electrode poisoning by adsorbed hydrogen, blocking the electrode surface for further reduction of N-containing species.

Electrochemical removal of nitrate and nitrite has been demonstrated in a laboratory scale flow reactor under different operating conditions (Chapter 5). On the two investigated types of cathode materials (Cu and CuSn), the concentration of nitrate was reduced electrochemically to the maximum permissible limit (50 mg/L in EU).

An identical quantity of nitrate, was reduced at the CuSn cathode below the permissible limit (99.5% conversion), in 18 h while at the Cu cathode the process needed 20 h. In both cases, as the current density increases the conversion efficiency increases, less time being needed to successfully reduce the nitrate. Comparisons between these two electrodes indicate definite advantages in using the CuSn alloy for nitrate and nitrite destruction. The energy consumption values, estimated for the tests performed within this thesis, are comparable and even smaller compared to literature data.

7. References

[1] Soares, M. I. M., Biological denitrification of groundwater. *Water, Air, and Soil Pollution* **2000,** 123, (1-4), 183-193.

[2] Schoeman, J. J.; Steyn, A., Nitrate removal with reverse osmosis in a rural area in South Africa. *Desalination* **2003,** 155, (1), 15-26.

[3] Hiscock, K. M.; Lloyd, J. W.; Lerner, D. N., Review of natural and artificial denitrification of groundwater. *Water Research* **1991,** 25, (9), 1099-1111.

[4] Katsounaros, I.; Dortsiou, M.; Kyriacou, G., Electrochemical reduction of nitrate and nitrite in simulated liquid nuclear wastes. *Journal of Hazardous Materials* **2009,** 171, (1-3), 323-327.

[5] Hobbs, D. T. In *Electrochemical treatment of liquid wastes*, Efficient separations and crosscutting program, technical exchange meeting, Gaithersburg, MD, USA, 1997; Gaithersburg, MD, USA, **1997**.

[6] Reyter, D.; Bélanger, D.; Roué, L., Study of the electroreduction of nitrate on copper in alkaline solution. *Electrochimica Acta* **2008,** 53, (20), 5977-5984.

[7] Katsounaros, I.; Kyriacou, G., Influence of the concentration and the nature of the supporting electrolyte on the electrochemical reduction of nitrate on tin cathode. *Electrochimica Acta* **2007,** 52, (23), 6412-6420.

[8] Mácová, Z.; Bouzek, K.; Šerák, J., Electrocatalytic activity of copper alloys for NO3-Reduction in a weakly alkaline solution: Part 2: Copper-tin. *Journal of Applied Electrochemistry* **2007,** 37, (5), 557-566.

[9] Polatides, C.; Kyriacou, G., Electrochemical reduction of nitrate ion on various cathodes - Reaction kinetics on bronze cathode. *Journal of Applied Electrochemistry* **2005,** 35, (5), 421-427.

[10] De, D.; Englehardt, J. D.; Kalu, E. E., Cyclic voltammetric studies of nitrate and nitrite ion reduction at the surface of iridium-modified carbon fiber electrode. *Journal of the Electrochemical Society* **2000,** 147, (11), 4224-4228.

[11] Low, C. T. J.; Walsh, F. C., The stability of an acidic tin methanesulfonate electrolyte in the presence of a hydroquinone antioxidant. *Electrochimica Acta* **2008,** 53, (16), 5280-5286.

[12] Oniciu L., Mureşan, L., *Electrochimie aplicată*. Presa Universitară Clujeană: Cluj-Napoca, Romania, **1998.**

[13] Grujicic, D.; Pesic, B., Electrodeposition of copper: The nucleation mechanisms. *Electrochimica Acta* **2002,** 47, (18), 2901-2912.

[14] Quemper, J. M.; Dufour-Gergam, E.; Frantz-Rodriguez, N.; Gilles, J. P.; Grandchamp, J. P.; Bosseboeuf, A., Effects of direct and pulse current on copper electrodeposition through photoresist molds. *Journal of Micromechanics and Microengineering* **2000,** 10, (2), 116-119.

[15] Torrent-Burgués, J.; Guaus, E.; Sanz, F., Initial stages of tin electrodeposition from sulfate baths in the presence of gluconate. *Journal of Applied Electrochemistry* **2002,** 32, (2), 225-230.

[16] Bennett, S., The electrodeposition of tin cadmium alloys. *Journal of the Electrodepositors' Technical Society* **1950,** 26, 107-118.

[17] Bălaj, F. M.; Imre-Lucaci, F.; Dorneanu, S. A.; Ilea, P.; Synthesis and characterisation of some metallic materials for nitrate reduction. *The 61st Annual Meeting of ISE – Electrochemistry from Biology to Physics*, Nice, France, **2010**, (Poster).

[18] Bălaj, F. M.; Dorneanu, S. A.; Imre-Lucaci, F.; Ilea, P.; Detection of electroactive products resulted from electrochemical nitrate reduction in alkaline media. *Studia Universitatis Babes-BolyaiChemia* **2009**, (SPEC. ISSUE 1), 127-134.

[19] Cuibus, F. M.; Ispas, A.; Bund, A.; Ilea, P.; Square wave voltammetric detection of electroactive products resulting from electrochemical nitrate reduction in alkaline media. *Journal of Electroanalytical Chemistry* **2012**, submitted.

[20] Bălaj, F. M.; Imre-Lucaci, F.; Dorneanu, S. A.; Ilea, P.; Detection of electroactive products resulted from electrochemical nitrate reduction in alkaline media. International conference *Journees d'Electrochimie*, Sinaia, Romania, **2009**, (Poster).

[21] Piela B.; Wrona, P. K., Oxidation of nitrites on solid electrodes I. Determination of the reaction mechanism on the pure electrode surface. *Journal of the Electrochemical Society* **2002,** 149, (2), E55-E63.

[22] Bălaj, F. M.; Dorneanu, S. A.; Ilea, P., Depoluarea electrochimică a apelor reziduale cu continut de nitrati. International conference *Corrosion and Anti-Corrosion Protection*, Cluj Napoca, Romania, **2009** (oral Presentation).

[23] Gadde, R. R.; Bruckenstein, S., The electroreduction of nitrite in 0.1 M HClO4 at platinum. *Journal of Electroanalytical Chemistry* **1974,** 50, (2), 163-174.

[24] Piela, B.; Wrona, P. K., Oxidation of Hydroxylamine on the Rotating Solid Electrodes: I. Oxidation of Hydroxylamine in Protonated Form. *Journal of the Electrochemical Society* **2004,** 151, (2), E69-E79.

[25] Kelter P.; Mosher, M.; Schott, A., *Chemistry: The practical Science, Media Enhanced Edition*. Cengage Learning Inc., USA, **2009.**

[26] Cuibus, F. M.; Ispas, A.; Bund, A.; Ilea, P.; Square Wave Voltammetry for the Detection of Electroactive Products Resulting from Nitrate Reduction at a Copper-Tin Alloy Electrode. International conference *Engineering of Functional Interfaces*, Linz, Austria, **2011** (Poster).

[27] Reyter D.; Odziemkowski, M.; Ɓlanger, D.; Roú, L., Electrochemically activated copper electrodes: Surface characterization, electrochemical behavior, and properties for the electroreduction of nitrate. *Journal of the Electrochemical Society* **2007,** 154, (8), K36-K44.

[28] Cattarin, S., Electrochemical reduction of nitrogen oxyanions in 1 M sodium hydroxide solutions at silver, copper and CuInSe2 electrodes. *Journal of Applied Electrochemistry* **1992,** 22, (11), 1077-1081.

[29] Horanyi, G.; Rizmayer, E. M., Electrocatalytic reduction of NO2- and NO3- ions at a platinized platinum electrode in alkaline medium. *Journal of Electroanalytical Chemistry* **1985,** 188, (1-2), 265-272.

[30] Bălaj, F. M.; Dorneanu, S. A.; Ispas, A.; Bund, A.; Ilea, P.; Detection of products resulting from nitrate reduction in alkaline media by square wave voltammetry. International conference *Electrochemistry - From microscopic understanding to global impact*, Bochum, Germany, **2010** (Poster).

[31] Cuibus, F. M.; Dorneanu, S. A.; Ispas, A.; Bund, A.; Ilea, P.; Square Wave Voltammetry for the detection of electroactive products resulting from nitrate reduction at a Cu-Sn Alloy electrode. International conference *The 220th ECS Meeting*, Boston, MA, USA, **2011** (oral Presentation).

[32] Bouzek, K.; Paidar, M.; Sadílková, A.; Bergmann, H., Electrochemical reduction of nitrate in weakly alkaline solutions. *Journal of Applied Electrochemistry* **2001,** 31, (11), 1185-1193.

[33] Gootzen, J. F. E.; Peeters, P. G. J. M.; Dukers, J. M. B.; Lefferts, L.; Visscher, W.; Van Veen, J. A. R., The electrocatalytic reduction of NO-3 on Pt, Pd and Pt + Pd electrodes activated with Ge. *Journal of Electroanalytical Chemistry* **1997,** 434, (1-2), 171-183.

[34] Endo, K.; Katayama, Y.; Miura, T., A rotating disk electrode study on the ammonia oxidation. *ElectrochimicaActa***2005,** 50, (11), 2181-2185.

[35] Prasad, P. K. R.; Priya, M. N.; Palanivelu, K., Nitrate removal from groundwater using electrolytic reduction method. *Indian Journal of Chemical Technology* **2005,** 12, (2), 164-169.

[36] Koparal, A. S.; Öütveren, U. B., Removal of nitrate from water by electroreduction and electrocoagulation. *Journal of Hazardous Materials* **2002,** 89, (1), 83-94.

[37] Reyter D.; Bélanger, D.; Roué, L., Optimization of the cathode material for nitrate removal by a paired electrolysis process. *Journal of Hazardous Materials* **2011,** 192, (2), 507-513.